Electronic Supplementary Information

A red ambient afterglow material with lifetime of 0.5 s and efficiency over 12%

Xingsha Shen,‡[a] Yanju Luo,‡[b] Kuan Chen,[a] Caixia Fu,[a] Ruyi Liu,[a] Yan Huang,[a]* Kaiqun Wu,[a] Juan Luo[a] and Zhiyun Lu[a]*

a. *Key Laboratory of Green Chemistry and Technology (Ministry of Education), College of Chemistry, Sichuan University, Chengdu 610064, China. E-mail: huangyan@scu.edu.cn; luzhiyun@scu.edu.cn.*

b. *Analytical & Testing Centre, Sichuan University, Chengdu 610064, China.*

Table of Contents

I. Experimental Section

Chemical Reagents and Materials

Unless otherwise described, all the reagents and anhydrous solvents were purchased from commercial sources and used without further purification. All the solvents used in photophysical measurements were of analytical grade and freshly distilled before use.

Instruments and Measurements

^{1}H NMR and ^{13}C NMR spectra were recorded on a Bruker Advanced II (400 MHz) spectrometer at 400 and 100 MHz in $CDCl_3$ and DMSO-d_6 as solvents and tetramethylsilane (TMS) as internal standard. High resolution MS spectra were measured on a Q-TOF Premier ESI mass spectrometer (Micromass, Manchester, UK). UV-vis absorption spectra were obtained on a UV 2600 spectrophotometer. Steady-state and delayed photoluminescence (PL) emission spectra were recorded on a HORIBA Jobin Yvon Fluoromax+ fluorescence spectrophotometer. PL quantum yields (QY) were collected on a HORIBA Jobin Yvon Fluorolog-3 fluorescence spectrometer equipped with an integrating sphere (IS80 from Labsphere) and a digital photometer (S370 from UDT) under ambient conditions. PL lifetimes were measured by a time-correlated single-photon counting (TCSPC) system using a HORIBA Jobin Yvon Fluorolog-3 fluorescence spectrometer. The concentration of solution samples for photophysical measurements was 1×10^{-6} M.

The total quantum yield (φ_{Total}) was measured by the matching integrating sphere under a hypoxic atmosphere. The phosphorescence quantum yield (φ_{Phos}) was calculated according to the following formula:

$$\varphi_{Phos} = \frac{B}{A} \times \varphi_{Total}$$

In the formula, A, B, and φ_{Total} are the integrated absolute area of the total luminescence spectra and phosphorescence spectra, and the total quantum yield, respectively. The total luminescence spectra of these samples were acquired using a flash xenon lamp as the excitation source, with excitation/emission slits of 3 nm/3 nm, sample window

of 100 ms, flash counts of 500, initial delay time of 0 ms, and flash interval of 121 ms. The phosphorescence spectra were acquired using a flash xenon lamp as the excitation source, with excitation/emission slits of 3 nm/3 nm, sample window of 99.95 ms, flash counts of 500, initial delay time of 0.05 ms, and flash interval of 121 ms.

Photophysical rate constant data acquisition

Based on the experimental data of φ_{Fluo}, φ_{Phos}, τ_{Fluo} and τ_{Phos}, the rate constants of different photophysical processes were calculated according to Equations S1~S5 based on the assumption that the T_1 exciton loss in PMMA matrix is the only non-radiative pathway (*i.e.*, $k_{nr,S} = 0$ and hence $\varphi_{nr,S} = 0$).

$$\varphi_{ISC} = 1 - \varphi_{Fluo} \tag{S1}$$

$$k_{r,Fluo} = \frac{\varphi_{Fluo}}{\tau_{Fluo}} \tag{S2}$$

$$k_{r,Phos} = \frac{\varphi_{Phos}}{\tau_{Phos}\varphi_{ISC}} \tag{S3}$$

$$k_{ISC} = \frac{\varphi_{ISC}}{\tau_{Fluo}} \tag{S4}$$

$$k_{nr,T} = \frac{1}{\tau_{Phos}} - k_{r,Phos} \tag{S5}$$

Theoretical calculations

The molecular geometries of **Cz**, **αCb**, **βCb**, **γCb**, **δCb**, **AP**, **PhAP**, and **γCbPhAP** at ground state were optimized using the density functional theory (DFT) method at the B3LYP/6-31g (d) level in the Gaussian 16 program. On the basis of the ground state geometries, exciton energies in the lowest singlet state (S_1), the lowest triplet state (T_1) and higher-lying triplet states (T_n) that are close to S_1 state were estimated through a combination of time-dependent DFT (TD-DFT) and PBE0 at the 6-31g (d) level. Spin-orbit coupling matrix elements (SOCME) between S_1 and corresponding triplet excited states were calculated with spin-orbit mean-field (SOMF) methods. Natural transition orbital (NTO) analysis was performed based on the TD-DFT results and subsequently

visualized via Gaussview (5.0).

Preparation of film samples

Preparation of 2,8-bis(diphenylphosphoryl)dibenzo[*b*,*d*]thiophene (PPT) film samples for the photo-physics measurements: compound (**CzPhAP** or **γCbPhAP**, 6 mg) and PPT (94 mg) were dissolved in 10 mL 1,2-dichloroethane, then 100 μL solution was spin-casted onto a clean quartz substrate of at 500 rpm for 10 s and 1500 rpm for 30 s at room temperature under air conditions.

Preparation of film samples for RTP measurements: compound (**AP**, **PhAP** or **γCbPhAP**, 1 mg) and PMMA (M_w= 350000 g mol^{-1}, 99 mg) were dissolved in 5 mL 1,2-dichloroethane. PVA (M_w= 85000 g mol^{-1}, 1 g) was dissolved in deionized water (50 mL) by stirring at 95°C to 130°C for 3 hours. Firstly, 500 μL of PMMA: compound solution was drop-casted onto a clean quartz substrate with an area of 2 cm × 0.5 cm under argon conditions. After the evaporation of 1,2-dichloroethane, 200 μL of PVA solution was drop-casted on the PMMA-based film to form an oxygen-barrier layer.

Synthesis and characterization

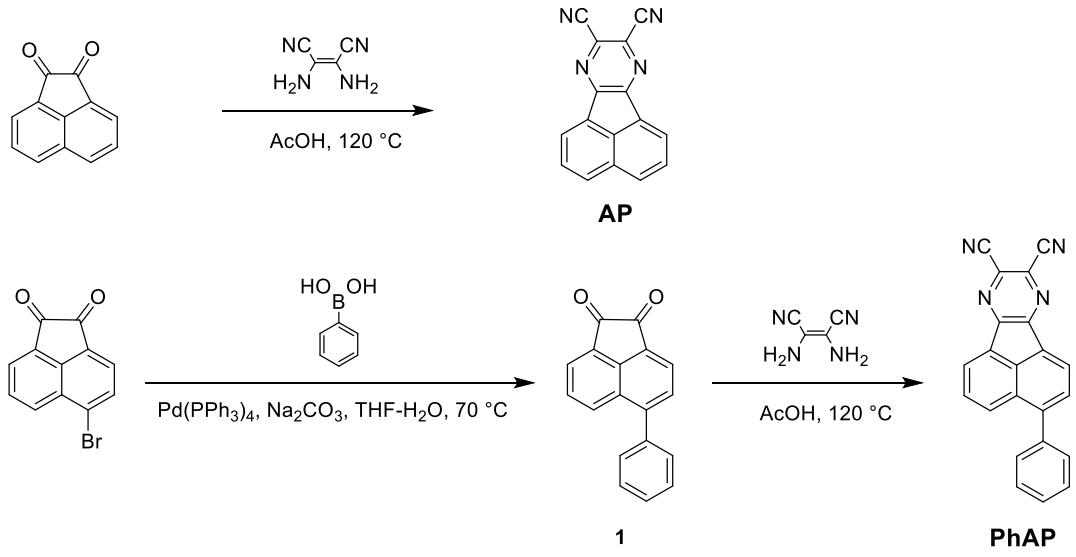

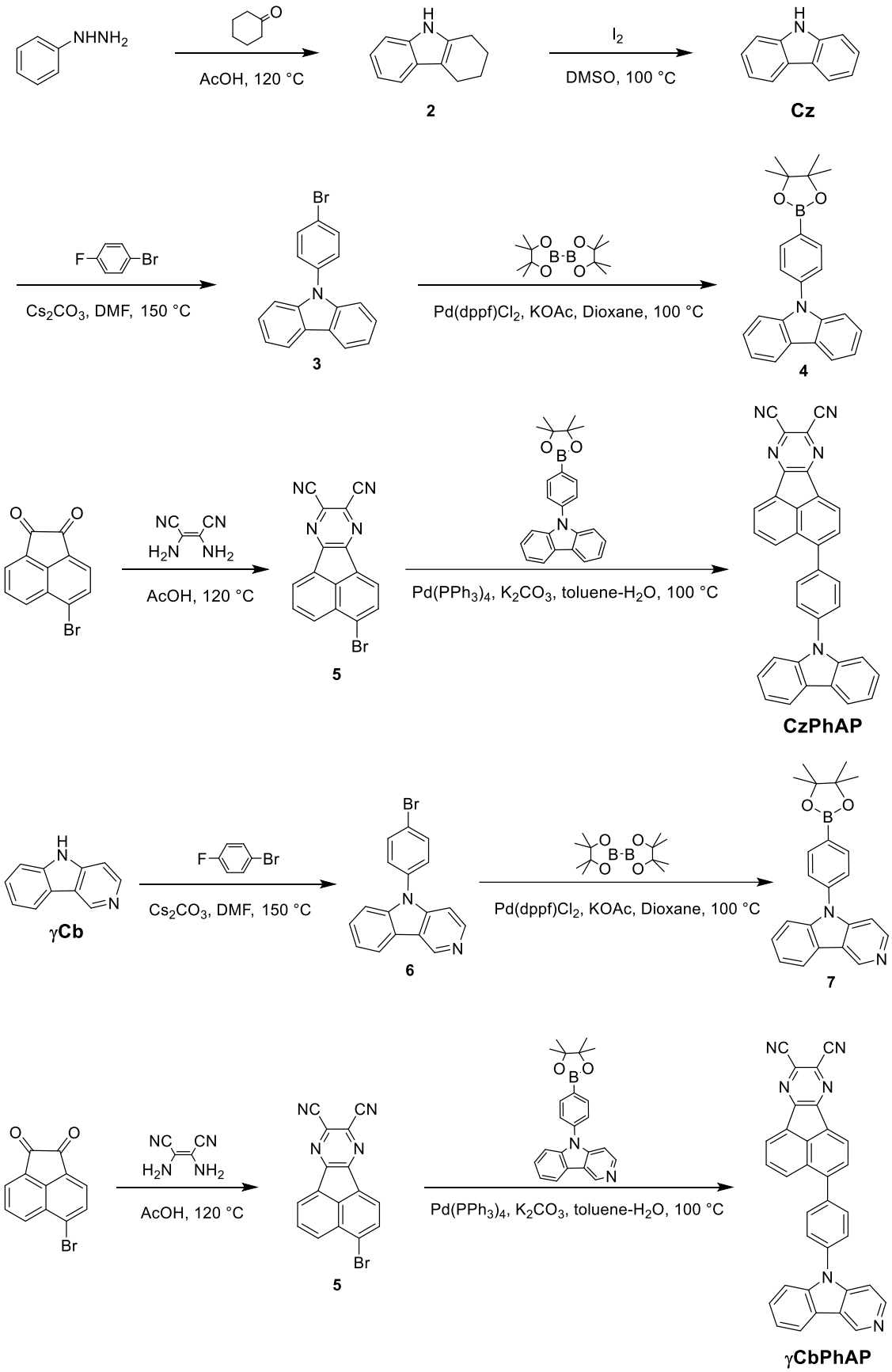

Scheme S1 The synthetic routes of **AP**, **PhAP**, **CzPhAP** and **γCbPhAP**.

Synthesis of acenaphtho[1,2-*b*]pyrazine-8,9-dicarbonitrile (AP)

Acenaphthylene-1,2-dione (500 mg, 2.75 mmol), 2,3-diaminomaleonitrile (297 mg, 2.75 mmol) and glacial acetic acid (10 mL) were added into a 50 mL three-necked flask and stirred at 120°C for 12 h under argon atmosphere. After cooling to room temperature, the mixture was poured into 100 mL of water. The separated solid was filtered off, washed with water, cool methanol, and then dried under a vacuum. The crude product was purified by column chromatography (silica gel) using petroleum ether: dichloromethane = 1:2 as eluent to give a yellow solid with a yield of 88%. ^{1}H NMR (400 MHz, $CDCl_3$) δ (ppm): 8.55 (d, *J* = 7.2 Hz, 2H), 8.33 (d, *J* = 8.4 Hz, 2H), 7.98 (t, *J* = 7.6 Hz, 2H). HRMS (ESI) m/z for $C_{16}H_7N_4^+$ $(M + H)^+$, calcd.: 255.0665, found: 255.0670. The solubility of the compound is poor, thus no ^{13}C NMR spectrum was measured.

Synthesis of 5-phenylacenaphthylene-1,2-dione (1)

5-bromoacenaphthylene-1,2-dione (522 mg, 2.00 mmol), phenylboronic acid (293 mg, 2.40 mmol), tetra (triphenylphosphine) palladium (115 mg, 0.10 mmol), anhydrous sodium carbonate (3180 mg, 30.00 mmol) and tetrahydrofuran-water mixed solvent (80 mL, V_{THF}/V_{H_2O} = 7:1) were added into a 250 mL three-necked flask and stirred at 70°C for 12 h under argon atmosphere. The reaction mixture was cooled to room temperature and THF was removed under vacuum conditions. Then the mixture was poured into water, followed by extraction with DCM (100 mL × 3). The resultant organic phase was washed with brine, and dried over anhydrous Na_2SO_4. After the removal of the solvent, the crude product was purified by column chromatography (silica gel) using petroleum ether: dichloromethane = 2:3 as eluent to give a yellow solid with a yield of 80%. ^{1}H NMR (400 MHz, $CDCl_3$) δ (ppm): 8.37 (dd, J_1 = 8.0 Hz, J_2 = 0.8 Hz, 1H), 8.19 (d, *J* = 7.2 Hz, 1H), 8.13 (dd, J_1 = 6.8 Hz, J_2 = 0.8 Hz, 1H), 7.83 (t, *J* = 7.6 Hz, 1H), 7.82 (d, *J* = 7.2 Hz, 1H), 7.63-7.52 (m, 5H).

Synthesis of 3-phenylacenaphtho[1,2-*b*]pyrazine-8,9-dicarbonitrile (PhAP)

1 (335 mg, 1.30 mmol), 2,3-diaminomaleonitrile (141 mg, 1.30 mmol) and glacial acetic acid (10 mL) were added into a 50 mL three-necked flask and stirred at 120°C for 12

h under argon atmosphere. After cooling to room temperature, the mixture was poured into 100 mL of water. The separated solid was filtered off, washed with water, cool methanol, and then dried under a vacuum. The crude product was purified by column chromatography (silica gel) using petroleum ether: dichloromethane = 1:2 as eluent to give a yellowish-green solid with a yield of 72%. ^{1}H NMR (400 MHz, $CDCl_3$) δ (ppm): 8.58 (t, J = 7.6 Hz, 2H), 8.41 (dd, J_1 = 8.4 Hz, J_2 = 0.8 Hz, 1H), 7.96 (t, J = 8.4 Hz, 1H), 7.95 (d, J = 7.6 Hz, 1H), 7.66-7.54 (m, 5H). ^{13}C NMR (100 MHz, $CDCl_3$) δ (ppm): 154.3, 146.9, 138.0, 135.8, 132.1, 130.2, 130.0, 129.4, 128.9, 128.8, 128.7, 128.3, 126.2, 126.1, 114.3. HRMS (ESI) m/z for $C_{22}H_{11}N_4^+$ $(M + H)^+$, calcd.: 331.0978, found: 331.0980.

Synthesis of 2,3,4,9-tetrahydro-1*H*-carbazole (2)

Phenylhydrazine (10.36 mL, 0.10 mol), cyclohexanone (10.36 mL, 0.10 mol) and acetic acid (120 mL) were added into a 250 mL three-necked flask and stirred at 120°C for 12 h. After cooling to room temperature, the mixture was poured into 500 mL water, and the precipitate was collected by filtration under a vacuum and washed with water to afford the crude product. Then the crude was recrystallized with methanol to finally obtain a white solid with a yield of 89%. ^{1}H NMR (400 MHz, $CDCl_3$) δ (ppm): 7.64 (s, 1H), 7.47 (dd, J_1 = 7.2 Hz, J_2 = 1.8 Hz, 1H), 7.28 (d, J = 7.6 Hz, 1H), 7.10 (td, J_1 = 8.0 Hz, J_2 = 1.6 Hz, 1H), 7.10 (td, J_1 = 8.4 Hz, J_2 = 1.2 Hz, 1H), 2.73 (m, 4H), 1.92 (m, 4H).

Synthesis of 9*H*-carbazole (Cz)

2 (1700 mg, 10.00 mmol), iodine (617 mg, 2.45 mmol), and dimethyl sulfoxide (40 mL) were added into a 250 mL three-necked flask and stirred at 100°C for 10 h. After the mixture was cooled down to room temperature, the reaction was quenched by the addition of con. HCl (2 mL) followed by stirring for 1 h, then the mixture was poured into an ice-cold saturated solution of sodium thiosulphate and stirred overnight at 5°C. The precipitate was collected by filtration under a vacuum and washed with water to afford the crude product. The crude product was purified by column chromatography (silica gel) using petroleum ether: ethyl acetate = 10:1 as eluent to give a white solid with a yield of 67%. ^{1}H NMR (400 MHz, DMSO-d_6) δ (ppm): 11.23 (s, 1H), 8.10 (dd, J_1

= 8.0 Hz, J_2 = 1.0 Hz, 2H), 7.48 (d, J = 8.0 Hz, 2H), 7.37 (dd, J_1 = 6.8 Hz, J_2 = 1.2 Hz, 2H), 7.15 (dd, J_1 = 7.6 Hz, J_2 = 0.8 Hz, 2H).

Synthesis of 9-(4-bromophenyl)-9*H*-carbazole (3)

1-bromo-4-fluorobenzene (1.31 mL, 11.96 mmol), **Cz** (500 mg, 2.99 mmol), cesium carbonate (3900 mg, 11.96 mmol), and *N*, *N*-dimethylformamide (10 mL) were added into a 100 mL Schlenk tube. The mixture was degassed through freeze-pump-thaw for three times, then stirred at 150°C for 24 h under argon. After being cooled down to room temperature, the mixture was poured into water, followed by extraction with DCM (100 mL × 3). The resultant organic phase was washed with brine, and dried over anhydrous Na_2SO_4. After the removal of the solvent, the crude product was purified by column chromatography (silica gel) using petroleum ether as eluent to give a white solid with a yield of 63%. ^{1}H NMR (400 MHz, $CDCl_3$) δ (ppm): 8.15 (d, J = 7.6 Hz, 2H), 7.74 (d, J = 8.4 Hz, 2H), 7.46 (d, J = 8.4 Hz, 2H), 7.42 (dd, J_1 = 7.2 Hz, J_2 = 1.4 Hz, 2H), 7.38 (d, J = 7.6 Hz, 2H), 7.31 (td, J_1 = 7.2 Hz, J_2 = 1.2 Hz, 2H).

Synthesis of 9-(4-(4,4,5,5-tetramethyl-1,3,2-dioxaborolan-2-yl)phenyl)-9*H*-carbazole (4)

3 (300 mg, 0.93 mmol), bis(pinacolato)diborane (470 mg, 1.86 mmol), Pd(dppf)Cl_2 (34 mg, 0.05 mmol), potassium acetate (275 mg, 2.79 mmol) and 1,4-dioxane (10 mL) were added into a 100 mL Schlenk tube. The mixture was degassed through freeze-pump-thaw for three times, then stirred at 100°C for 10 h under argon. After cooling down to room temperature, the mixture was poured into water. After extraction with DCM (100 mL × 3), the resultant organic phase was washed with brine, and dried over anhydrous Na_2SO_4. After the removal of the solvent, the crude product was purified by column chromatography (silica gel) using petroleum ether: ethyl acetate = 10:1 as eluent to give a white solid with a yield of 57%. ^{1}H NMR (400 MHz, $CDCl_3$) δ (ppm): 8.14 (d, J = 7.6 Hz, 2H), 8.06 (d, J = 8.4 Hz, 2H), 7.60 (d, J = 8.4 Hz, 2H), 7.45 (d, J = 8.4 Hz, 2H), 7.41 (td, J_1 = 6.8 Hz, J_2 = 1.2 Hz, 2H), 7.30 (td, J_1 = 6.8 Hz, J_2 = 1.2 Hz, 2H), 1.40 (s, 12H).

Synthesis of 3-bromoacenaphtho[1,2-*b*]pyrazine-8,9-dicarbonitrile (5)

5-bromoacenaphthylene-1,2-dione (522 mg, 2.00 mmol), 2,3-diaminomaleonitrile (216 mg, 2.00 mmol) and glacial acetic acid (10 mL) were added into a 50 mL three-necked flask and stirred at 120°C for 12 h under argon atmosphere. After cooling to room temperature, the mixture was poured into 100 mL of water. The separated solid was filtered off, washed with water, cool methanol, and then dried under a vacuum. The crude product was purified by column chromatography (silica gel) using petroleum ether: dichloromethane = 1:2 as eluent to give a yellow solid with a yield of 70%. ^{1}H NMR (400 MHz, DMSO-d_6) δ (ppm): 8.69 (dd, J_1 = 7.2 Hz, J_2 = 0.8 Hz, 1H), 8.47 (td, J_1 = 7.6 Hz, J_2 = 0.8 Hz, 2H), 8.33 (d, J = 7.6 Hz, 1H), 8.16 (td, J_1 = 7.6 Hz, J_2 = 1.2 Hz, 1H).

Synthesis of 3-(4-(9*H*-carbazol-9-yl)phenyl)acenaphtho[1,2-*b*]pyrazine-8,9-dicarbonitrile (CzPhAP)

4 (194 mg, 0.53 mmol), **5** (147 mg, 0.44 mmol), tetra (triphenylphosphine) palladium (25 mg, 0.02 mmol), anhydrous potassium carbonate (304 mg, 2.20 mmol) and toluene-water mixed solvent (6 mL, V_{Tol}/V_{H_2O}=3/1) were added into a 25 mL Schlenk tube. The mixture was degassed through freeze-pump-thaw for three times, then stirred at 100°C for 12 h under argon. After cooling down to room temperature, the mixture was poured into water, followed by extraction with DCM (100 mL × 3). The resultant organic phase was washed with brine, and dried over anhydrous Na_2SO_4. After the removal of the solvent, the crude product was purified by column chromatography (silica gel) using petroleum ether: dichloromethane = 1:2 as eluent to give an orange solid with a yield of 62%. ^{1}H NMR (400 MHz, $CDCl_3$) δ (ppm): 8.66 (d, J = 7.2 Hz, 1H), 8.62 (d, J = 7.2 Hz, 1H), 8.55 (d, J = 8.4 Hz, 1H), 8.20 (d, J = 8.0 Hz, 2H), 8.05 (m, 2H), 7.90 (d, J = 8.4 Hz, 2H), 7.85 (d, J = 8.4 Hz, 2H), 7.58 (d, J = 8.0 Hz, 2H), 7.48 (td, J_1 = 6.8 Hz, J_2 = 1.6 Hz, 2H), 7.36 (td, J_1 = 7.6 Hz, J_2 = 1.2 Hz, 2H). ^{13}C NMR (100 MHz, 1,2-dichlorobenzene-d_4) δ (ppm): 154.5, 154.1, 145.6, 140.6, 138.6, 136.9, 135.8, 134.2, 133.3, 132.9, 132.2, 131.9, 131.7, 131.0, 130.8, 130.6, 129.6, 129.4, 129.1, 129.0, 128.1, 128.0, 127.8, 127.7, 126.4, 126.1, 124.1, 120.8,

120.7. HRMS (ESI) m/z for $C_{34}H_{18}N_5^+$ $(M + H)^+$, calcd.: 496.1557, found: 496.1558.

Synthesis of 5-(4-bromophenyl)-5*H*-pyrido[4,3-*b*] indole (6)

1-bromo-4-fluorobenzene (0.52 mL, 4.76 mmol), **γCb** (200 mg, 1.19 mmol), cesium carbonate (1550 mg, 4.76 mmol) and *N*, *N*-dimethylformamide (5 mL) were added into a 25 mL Schlenk tube. The mixture was degassed through freeze-pump-thaw for three times, then stirred at 150°C for 24 h under argon. After being cooled down to room temperature, the mixture was poured into water, followed by extraction with DCM (100 mL × 3). The resultant organic phase was washed with brine, and dried over anhydrous Na_2SO_4. After the removal of the solvent, the crude product was purified by column chromatography (silica gel) using dichloromethane: ethyl acetate = 1:1 as eluent to give a brown solid with a yield of 47%. ^{1}H NMR (400 MHz, DMSO-d_6) δ (ppm): 9.47 (s, 1H), 8.49 (d, J = 5.6 Hz, 1H), 8.37 (d, J = 7.6 Hz, 1H), 7.89 (d, J = 8.4 Hz, 2H), 7.64 (d, J = 8.8 Hz, 2H), 7.53 (td, J_1 = 8.0 Hz, J_2 = 1.2 Hz, 1H), 7.45 (d, J = 8.4 Hz, 1H), 7.41 (d, J_1 = 7.6 Hz, J_2 = 1.2 Hz, 1H), 7.38 (td, J_1 = 7.6 Hz, J_2 = 1.2 Hz, 1H).

Synthesis of 5-(4-(4,4,5,5-tetramethyl-1,3,2-dioxaborolan-2-yl)phenyl)-5*H*-pyrido [4,3-*b*]indole (7)

6 (380 mg, 1.18 mmol), bis(pinacolato)diborane (599 mg, 2.36 mmol), Pd(dppf)Cl_2 (44 mg, 0.06 mmol), potassium acetate (347 mg, 3.54 mmol) and 1,4-dioxane (10 mL) were added into a 100 mL Schlenk tube. The mixture was degassed through freeze-pump-thaw for three times, then stirred at 100°C for 10 h under argon. After cooling down to room temperature, the mixture was poured into water. After extraction with DCM (100 mL × 3), the resultant organic phase was washed with brine, and dried over anhydrous Na_2SO_4. After the removal of the solvent, the crude product was purified by column chromatography (silica gel) using methanol: dichloromethane = 1:10 as eluent to give a white solid with a yield of 52%. ^{1}H NMR (400 MHz, $CDCl_3$) δ (ppm): 9.39 (s, 1H), 8.52 (d, J = 6.0 Hz, 1H), 8.22 (d, J = 8.0 Hz, 1H), 7.64 (t, J = 7.2 Hz, 2H), 7.55 (d, J = 7.2 Hz, 2H), 7.48 (d, J = 7.2 Hz, 1H), 7.44 (d, J = 8.0 Hz, 1H), 7.39 (t, J = 7.2 Hz, 1H), 7.30 (d, J = 5.6 Hz, 1H), 1.26 (s, 12H).

Synthesis of 3-(4-(5*H*-pyrido[4,3-*b*]indol-5-yl)phenyl)acenaphtho[1,2-b]pyrazine-8,9-dicarbonitrile (γCbPhAP)

7 (118 mg, 0.32 mmol), **5** (88 mg, 0.26 mmol), tetra (triphenylphosphine) palladium (15 mg, 0.01 mmol), anhydrous potassium carbonate (182 mg, 1.32 mmol) and toluene-water mixed solvent (4 mL, V_{Tol}/V_{H_2O}=3/1) were added into a 25 mL Schlenk tube. The mixture was degassed through freeze-pump-thaw for three times, then stirred at 100°C for 12 h under argon. After cooling down to room temperature, the mixture was poured into water, followed by extraction with DCM (100 mL × 3). The resultant organic phase was washed with brine, and dried over anhydrous Na_2SO_4. After the removal of the solvent, the crude product was purified by column chromatography (silica gel) using methanol: dichloromethane = 1:100 as eluent to give a yellow solid with a yield of 71%. ^{1}H NMR (400 MHz, $CDCl_3$) δ (ppm): 9.46 (s, 1H), 8.67 (d, *J* = 7.6 Hz, 1H), 8.63 (d, *J* = 6.8 Hz, 1H), 8.60 (d, *J* = 6.4 Hz, 1H), 8.50 (d, *J* = 8.4 Hz, 1H), 8.30 (d, *J* = 8.0 Hz, 1H), 8.07 (d, *J* = 7.2 Hz, 1H), 8.05 (t, *J* = 7.6 Hz, 1H), 7.96 (d, *J* = 8.0 Hz, 2H), 7.83 (d, *J* = 8.0 Hz, 2H), 7.63 (d, *J* = 4.0 Hz, 2H), 7.56 (d, *J* = 6.0 Hz, 1H), 7.51 (t, *J* = 7.6 Hz, 1H). ^{13}C NMR (100 MHz, 1,2-dichlorobenzene-d_4) δ (ppm): 154.5, 154.1, 145.9, 145.3, 144.6, 143.3, 140.6, 137.7, 137.3, 135.8, 134.2, 133.3, 132.9, 132.2, 132.1, 131.0, 130.9, 130.8, 130.6, 129.6, 128.0, 127.8, 126.8, 126.1, 126.0, 122.3, 122.0, 120.9, 120.6, 114.8, 110.4, 105.1. HRMS (ESI) m/z for $C_{33}H_{17}N_6^+$ $(M + H)^+$, calcd.: 497.1509, found: 497.1510.

II. Supplementary Figures

Summary of reported red UORTP materials (λ_{Phos} ≥ 600 nm, τ_{Phos} ≥ 0.3 s)

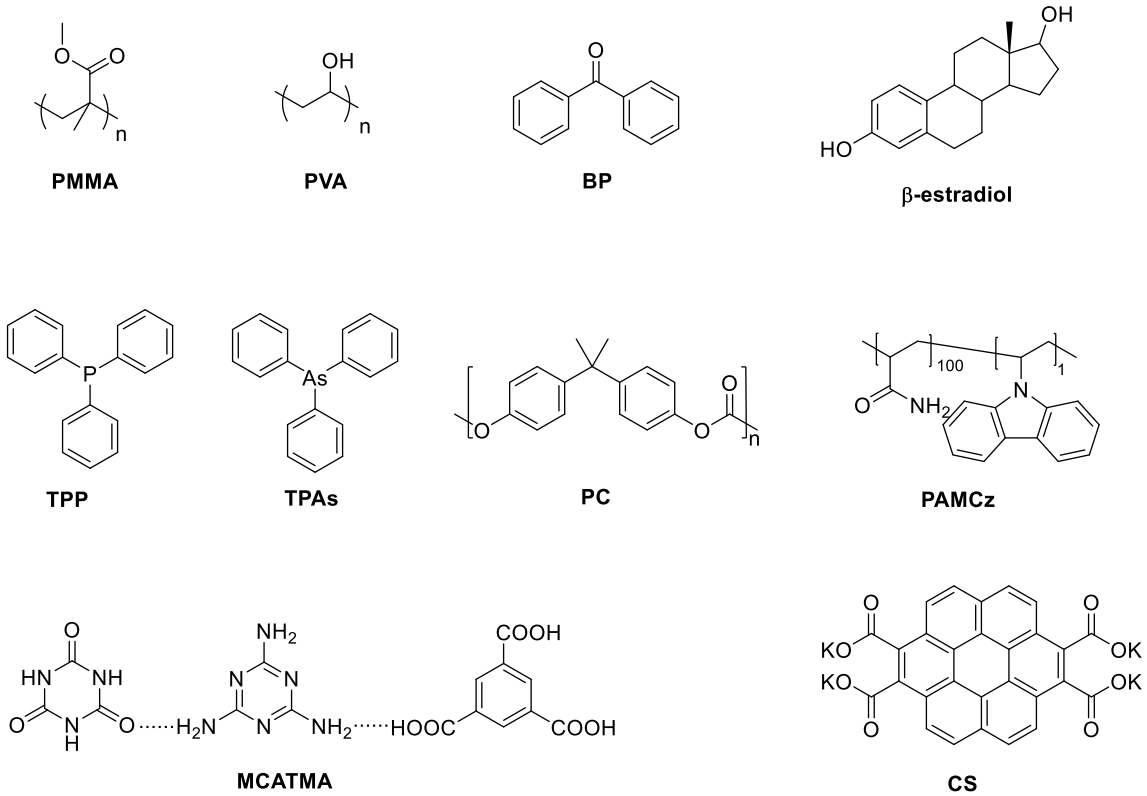

Fig. S1 Matrix structure.

Table S1 Photophysical properties of the red UORTP materials with τ_{Phos} ≥ 0.3 s.

Compound	Matrix	$\lambda_{Phos}/\lambda_{Afterglow}$ (nm)	$\tau_{Phos}/\tau_{Afterglow}$ (s)	$\varphi_{Phos}/\varphi_{Afterglow}$ (%)	Ref.
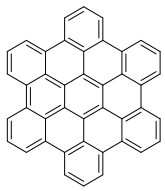	**PC**	625	4.00	11.87	1
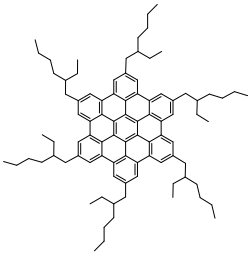	**β-estradiol**	628	3.90	2.6	2

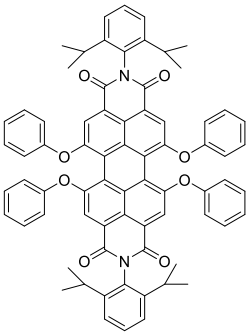	**PMMA**	650	2.80	-	1
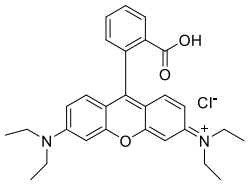	**PAMCz**	620	2.20	-	3
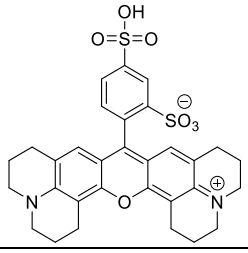	**CS/PVA**	615	2.15	-	4
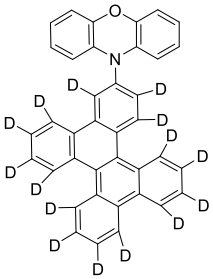	**β-estradiol**	624	1.80	16.1	5
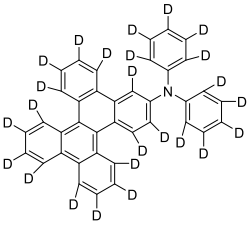	**β-estradiol**	625	1.12	5.3	6
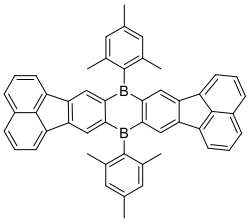	**PMMA**	614	0.76	2.9	7
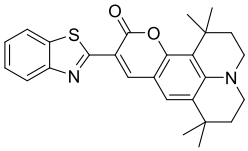	**MCATMA**	600	0.63	-	8

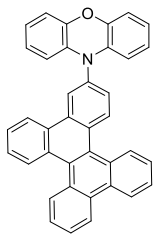	**β-estradiol**	626	0.61	6.6	5
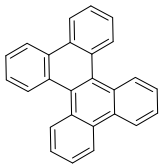	**β-estradiol**	626	0.58	2.9	5
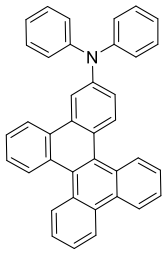	**β-estradiol**	632	0.49	3.9	5
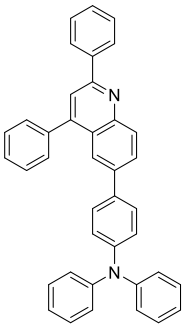	**TPAs**	605	0.47	10.9	9
	TPP	608	0.46	9.3	9
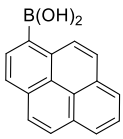	**PVA**	610	0.34	13.1	10
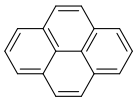	**BP**	600	0.33	9.2	11
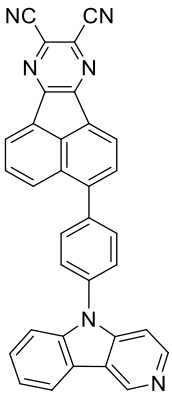	**PMMA**	**609**	**0.50**	**12.2**	**This work**

Photophysical properties in dilute solution

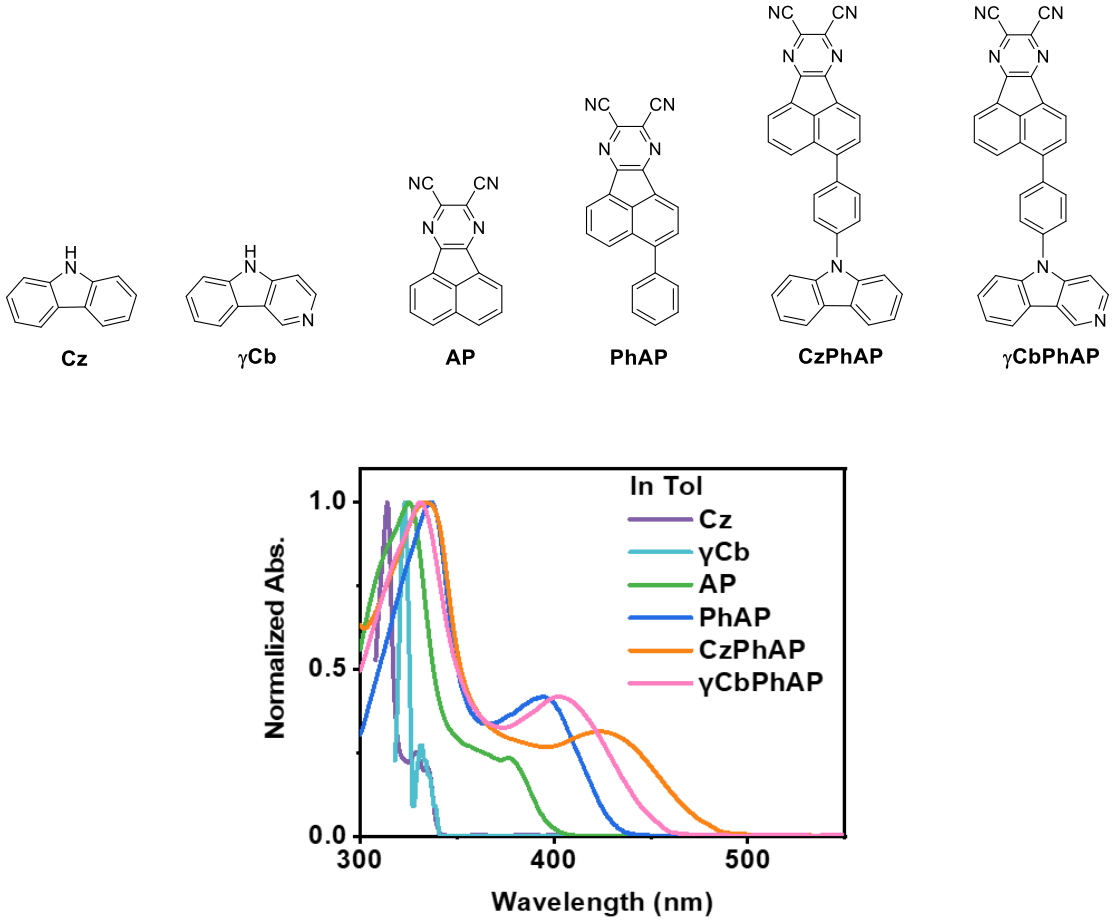

Fig. S2 UV-vis absorption spectra of **Cz**, **γCb**, **AP**, **PhAP**, **CzPhAP** and **γCbPhAP** in toluene under ambient conditions (1×10^{-5} M).

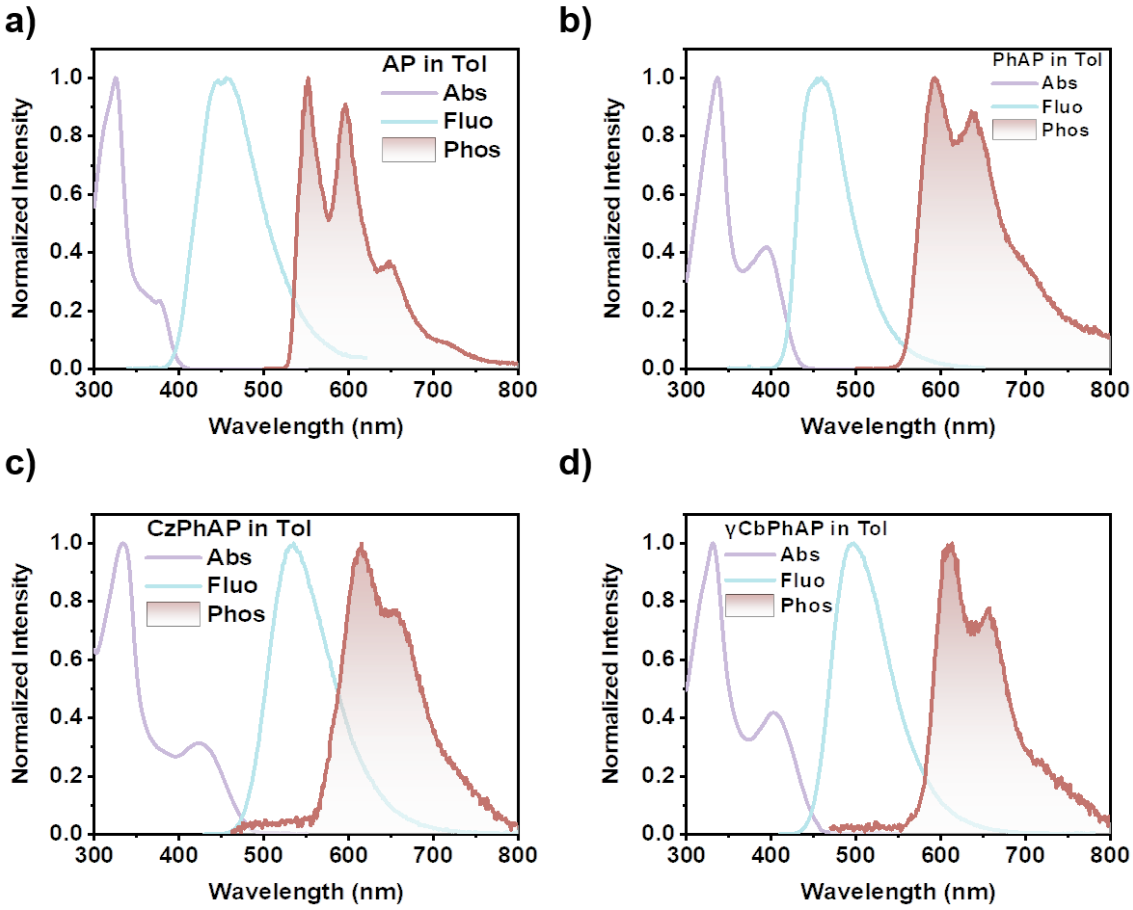

Fig. S3 UV-vis absorption (Abs) spectra, fluorescence (Fluo) spectra in toluene at RT, and phosphorescence (Phos) spectra (delay time: 10 ms, λ_{ex} = 330 nm) in toluene (1 × 10^{-6} M) at 77 K of a) **AP**; b) **PhAP**; c) **CzPhAP**; d) **γCbPhAP**.

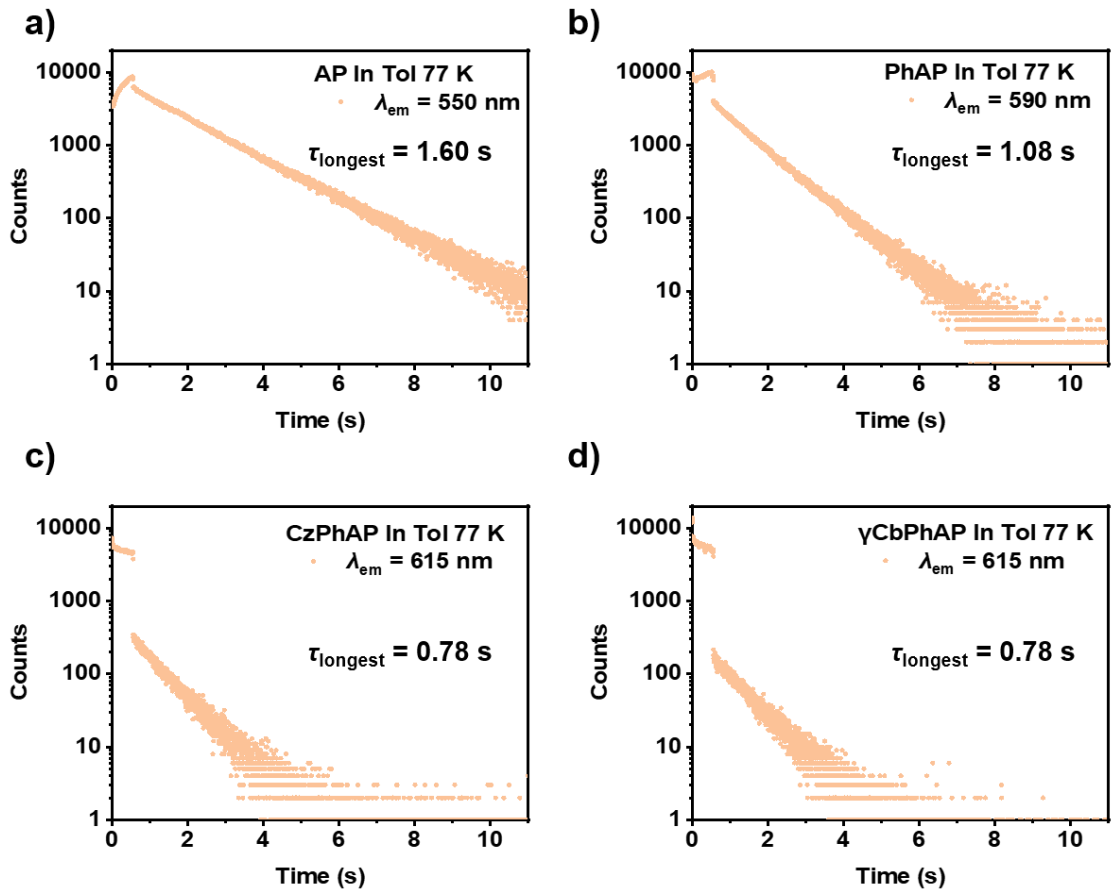

Fig. S4 Phosphorescence decay profiles of a) **AP**; b) **PhAP**; c) **CzPhAP**; and d) **γCbPhAP** in toluene (1×10^{-6} M, λ_{ex} = 355 nm) at 77 K.

Table S2 The fitting results of phosphorescence decay curves of **AP**, **PhAP**, **CzPhAP**, and **γCbPhAP** in toluene (1×10^{-6} M, λ_{ex} = 355 nm) at 77 K.

Compound	λ_{em}	Lifetime	χ^2
AP	550 nm	τ = 1.60 s	1.92
PhAP	590 nm	τ_1 = 0.07 s τ_2 = 0.66 s τ_3 = 1.08 s	1.06
CzPhAP	615 nm	τ_1 = 0.30 ms τ_2 = 0.21 s τ_3 = 0.78 s	1.01
γCbPhAP	615 nm	τ_1 = 0.62 ms τ_2 = 0.22 s τ_3 = 0.78 s	1.00

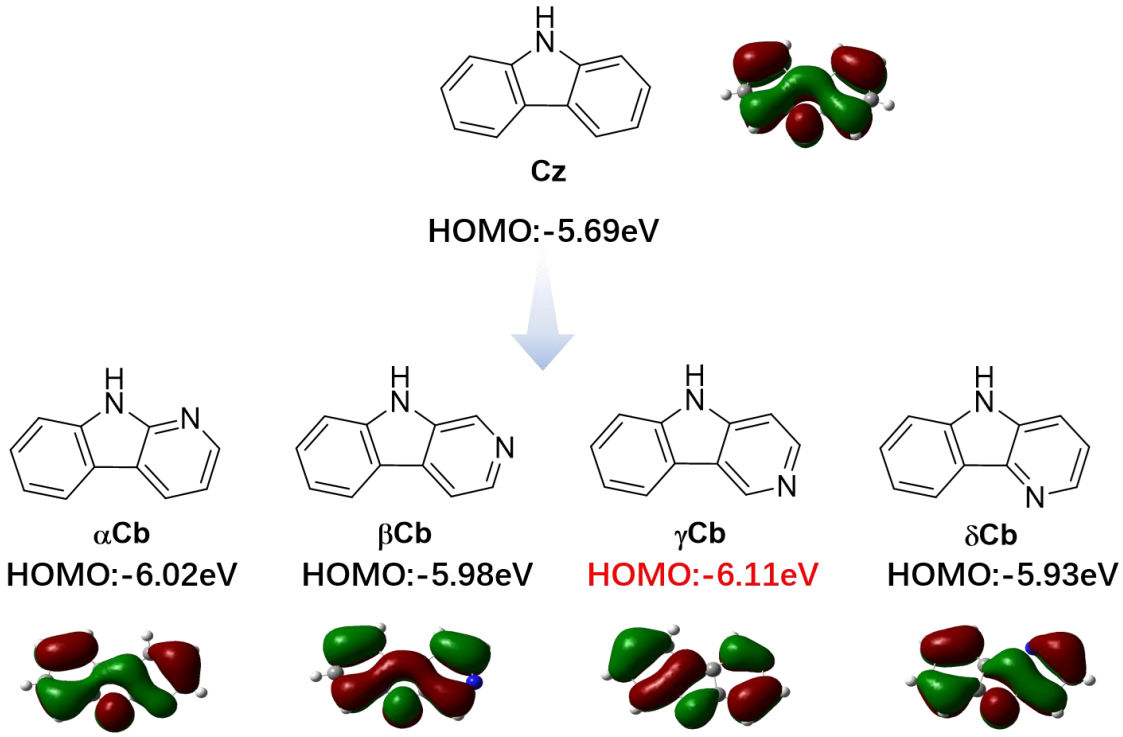

Fig. S5 Calculated energy level and contour plots of HOMO of **Cz**, **αCb**, **βCb**, **γCb**, and **δCb**.

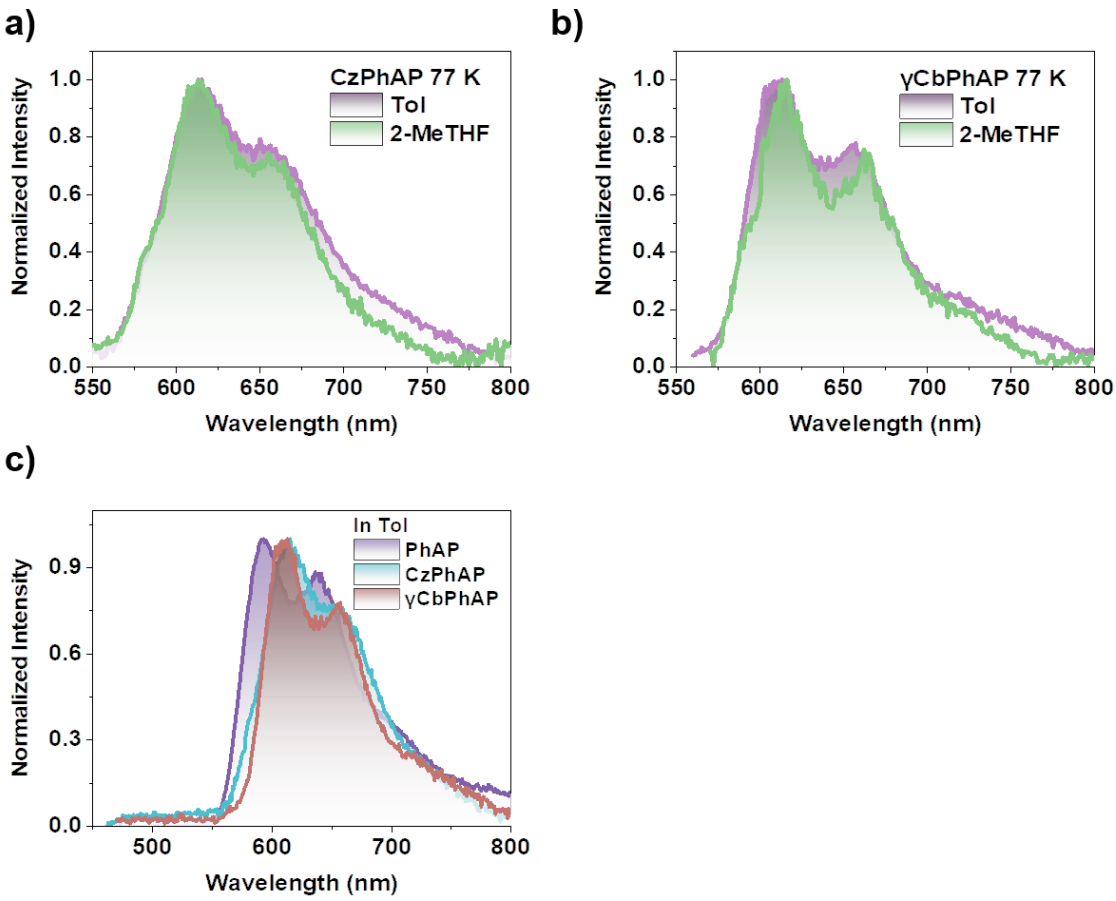

Fig. S6 Phosphorescence spectra (delay time: 10 ms, λ_{ex} = 330 nm) of a) **CzPhAP** and b) **γCbPhAP** in toluene (Tol) and 2-methyltetrahydrofuran (2-MeTHF) (1 × 10^{-6} M) at 77 K; c) Phosphorescence spectra (delay time: 10 ms, λ_{ex} = 330 nm) of **PhAP**, **CzPhAP** and **γCbPhAP** in toluene (1 × 10^{-6} M) at 77 K.

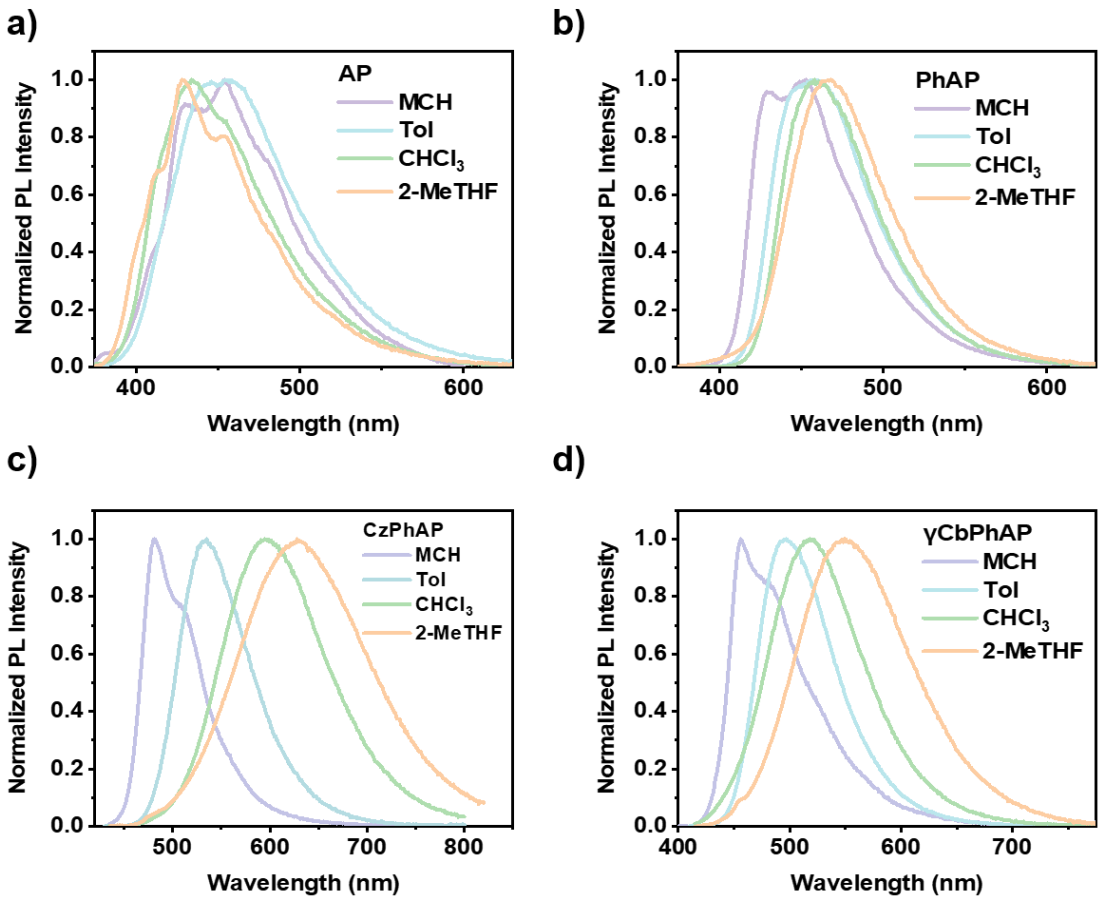

Fig. S7 PL emission spectra of a) **AP**; b) **PhAP**; c) **CzPhAP**; and d) **γCbPhAP** in methylcyclohexane (MCH), toluene (Tol), chloroform ($CHCl_3$) and 2-methyltetrahydrofuran (2-MeTHF) at RT under ambition conditions. (1×10^{-6} M, **AP** and **PhAP**: λ_{ex} = 330 nm, **CzPhAP**: λ_{ex} = 420 nm, **γCbPhAP**: λ_{ex} = 400 nm)

Photophysical properties in 6 wt% PPT film

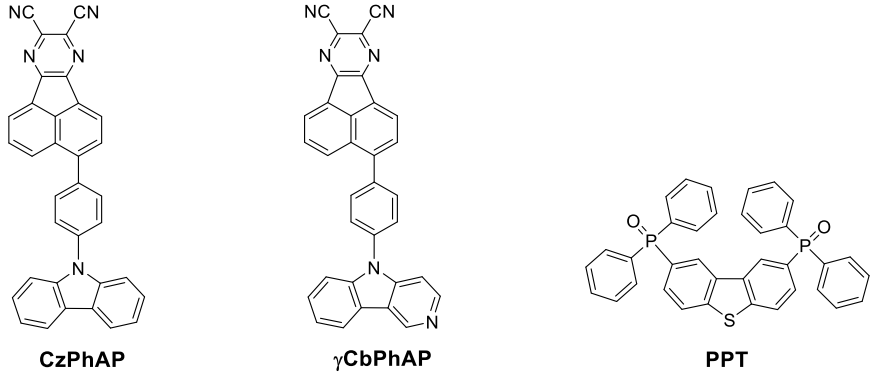

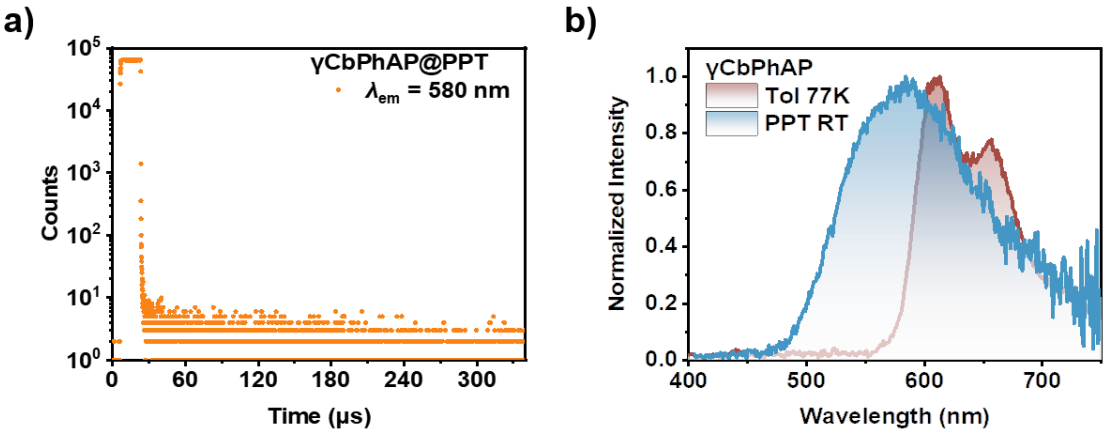

Fig. S8 a) Time-resolved PL decay profiles of **γCbPhAP** in PPT (doping ratio: 6 wt%, λ_{ex} = 370 nm) at RT under air conditions. b) Time-resolved PL spectra of **γCbPhAP** in Tol (1 × 10^{-6} M, delay time: 10 ms, λ_{ex} = 330 nm) at 77 K and in PPT (doping ratio: 6 wt%, delay time: 0.05 ms, λ_{ex} = 330 nm) at RT under nitrogen conditions.

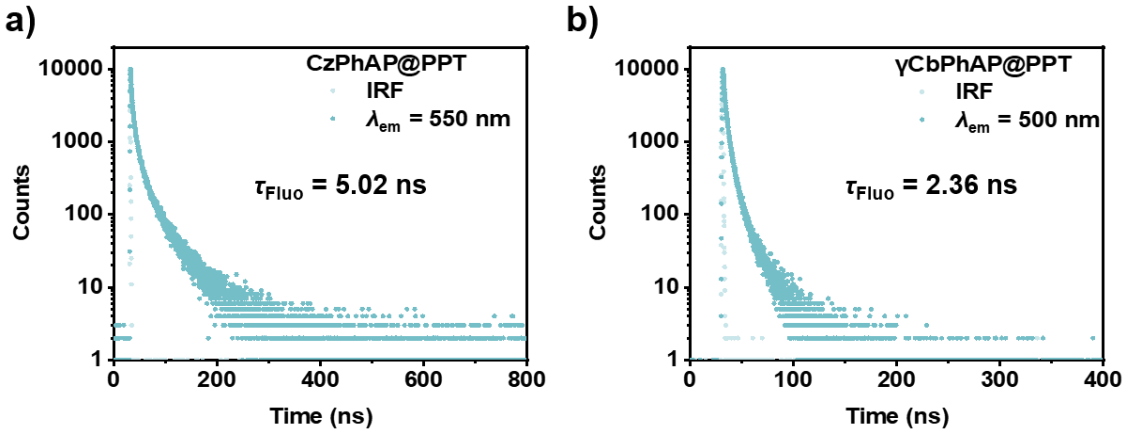

Fig. S9 Fluorescence decay profiles in PPT (doping ratio: 6 wt%, λ_{ex} = 370 nm) under ambient conditions of a) **CzPhAP**; and b) **γCbPhAP**.

Table S3 The fitting results of PL decay curves of **CzPhAP**@PPT and **γCbPhAP**@PPT (λ_{ex} = 370 nm) under ambient conditions.

Compound	λ_{em}	Lifetime	χ^2
CzPhAP	550 nm	τ_1 = 1.91 ns τ_2 = 10.20 ns τ_3 = 48.52 ns	1.01
	600 nm	τ_1 = 0.40 ms τ_2 = 0.01 s τ_3 = 0.07 s	1.15
γCbPhAP	500 nm	τ_1 = 1.04 ns τ_2 = 4.33 ns τ_3 = 16.80 ns	1.01
	580 nm	τ_1 = 95.12 μs τ_2 = 0.03 s τ_3 = 0.15 s	1.01

Photophysical properties in 1 wt% dope-casted PMMA film

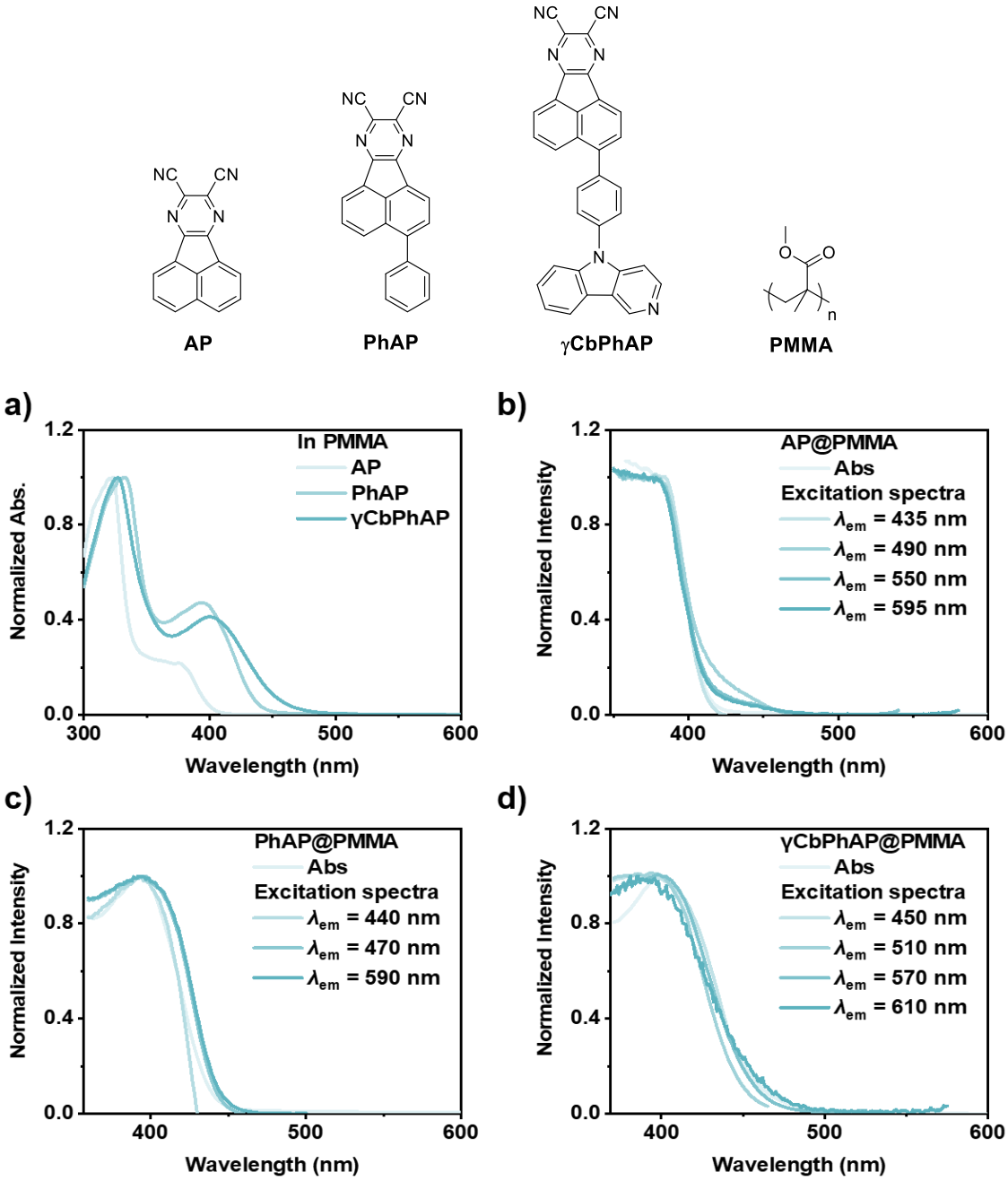

Fig. S10 a) UV-vis absorption spectra of **AP**, **PhAP**, **γCbPhAP** in PMMA matrix (doping ratio: 1 wt%). UV-vis absorption spectra and PL excitation spectra in PMMA matrix (doping ratio: 1 wt%) of b) **AP**; c) **PhAP**; and d) **γCbPhAP**.

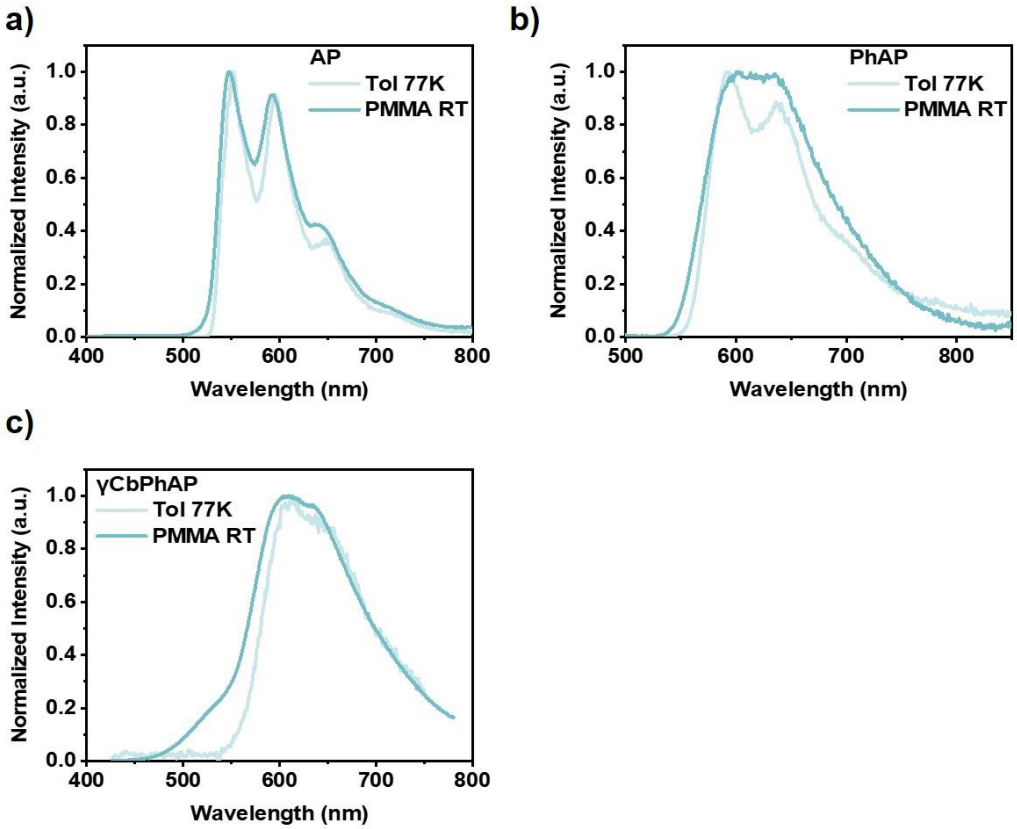

Fig. S11 Phosphorescence spectra (delay time: 10 ms) in toluene at 77 K and in PMMA at RT (doping ratio: 1 wt%) under ambient conditions of a) **AP** (λ_{ex} = 330 nm); b) **PhAP** (λ_{ex} = 330 nm); c) **γCbPhAP** (λ_{ex} = 400 nm).

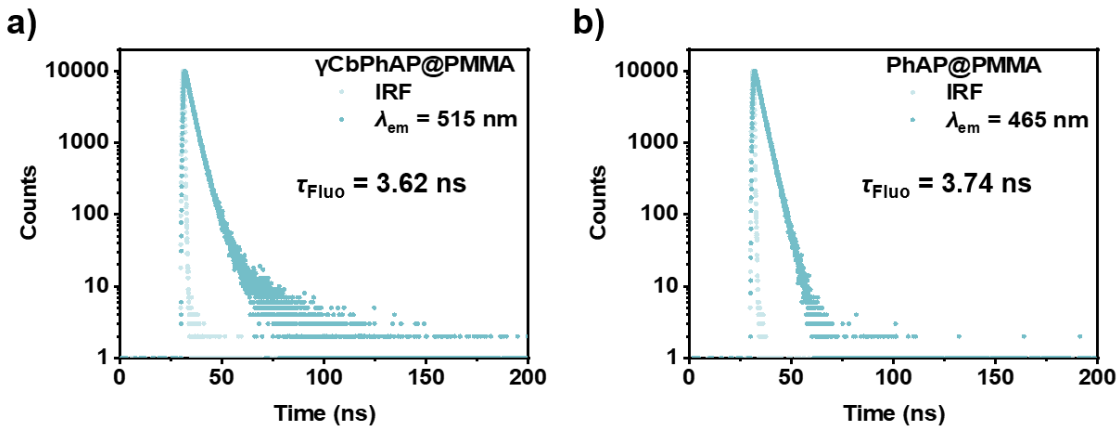

Fig. S12 Fluorescence decay profiles in PMMA (doping ratio: 1 wt%, λ_{ex} = 370 nm) under ambient conditions of a) **γCbPhAP**; b) **PhAP**.

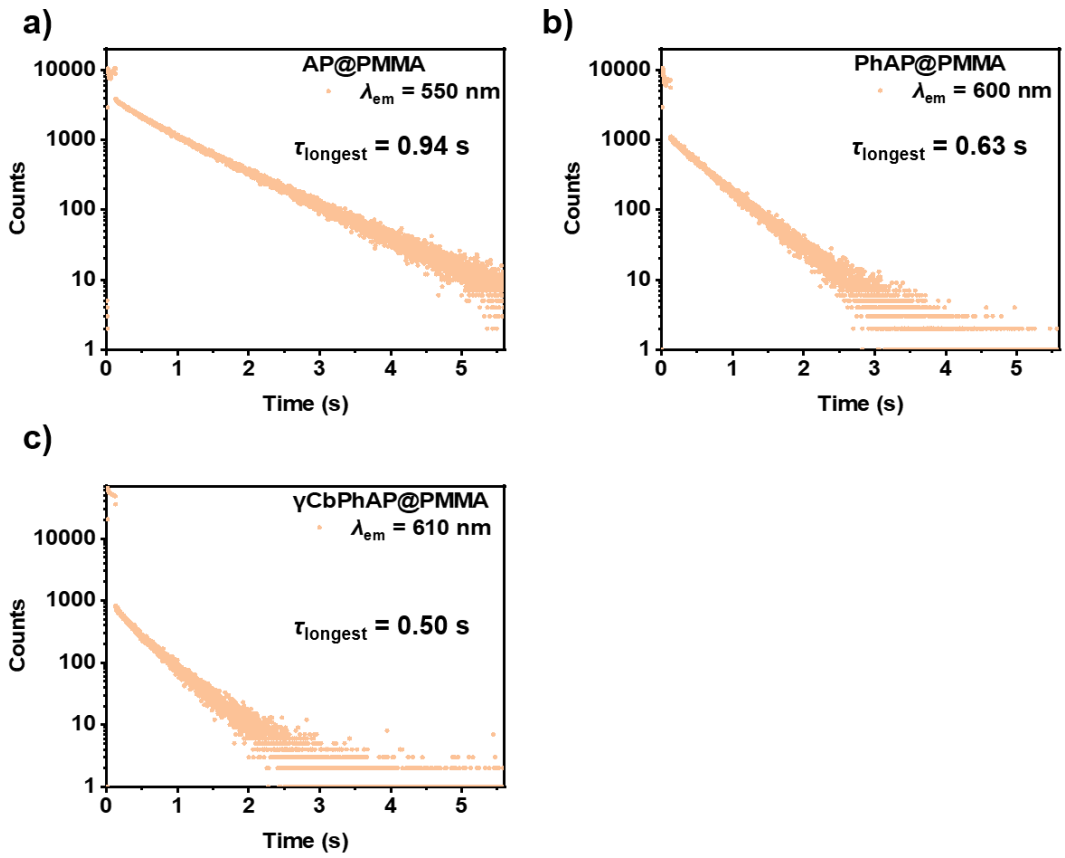

Fig. S13 Phosphorescence decay profiles in PMMA (doping ratio: 1 wt%, λ_{ex} = 370 nm) under ambient conditions of a) **AP**; b) **PhAP**; c) **γCbPhAP**.

Table S4 The fitting results of phosphorescence decay curves of **AP**@PMMA, **PhAP**@PMMA and **γCbPhAP**@PMMA (λ_{ex} = 370 nm) under ambient conditions.

Compound	λ_{em}	Lifetime	χ^2
AP	550 nm	τ_1 = 0.62 ms τ_2 = 0.42 s τ_3 = 0.94 s	1.01
PhAP	600 nm	τ_1 = 0.31 ms τ_2 = 0.39 s τ_3 = 0.63 s	1.01
γCbPhAP	610 nm	τ_1 = 0.20 ms τ_2 = 0.21 s τ_3 = 0.50 s	1.00

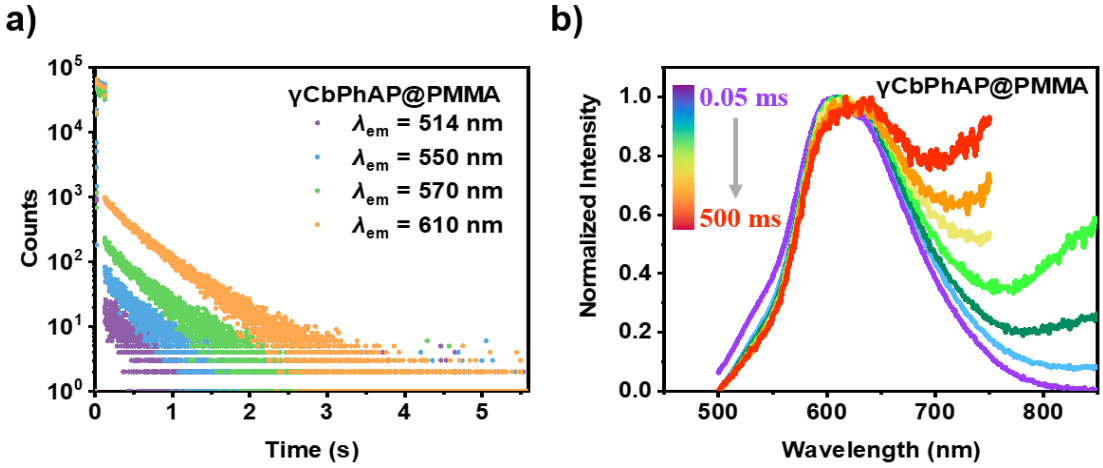

Fig. S14 a) Transient PL decay profiles, and b) delayed PL spectra of **γCbPhAP**@PMMA under ambient conditions (doping ratio: 1 wt%, λ_{ex} = 370 nm).

Table S5 The fitting results of PL decay curves of **γCbPhAP**@PMMA at different monitored λ_{em} under ambient conditions (λ_{ex} = 370 nm).

λ_{em}	Lifetime	Weight	χ^2
514 nm	τ_1 = 0.05 ms	99.8%	1.00
	τ_2 = 0.02 s	0.1%	
	τ_3 = 0.26 s	0.1%	
550 nm	τ_1 = 0.05 ms	99.7%	1.03
	τ_2 = 0.05 s	0.1%	
	τ_3 = 0.33 s	0.2%	
570 nm	τ_1 = 0.20 ms	99.3%	0.99
	τ_2 = 0.13 s	0.2%	
	τ_3 = 0.44 s	0.5%	
610 nm	τ_1 = 0.20 ms	97.3%	1.01
	τ_2 = 0.21 s	0.2%	
	τ_3 = 0.50 s	2.5%	

As shown in the above **Fig. S14a** and **Table S5**, the PL at 514 nm indeed show long-lived species ($\tau_{longest}$ = 0.26 s), validating the presence of ultra-long TADF species in this sample. Nevertheless, evidenced by **Fig. S14a** and **Fig. S14b**, the relative content of the DF species is relatively low, indicative of the phosphorescence-dominated nature of the afterglow of **γCbPhAP**@PMMA.

Theoretical calculation results

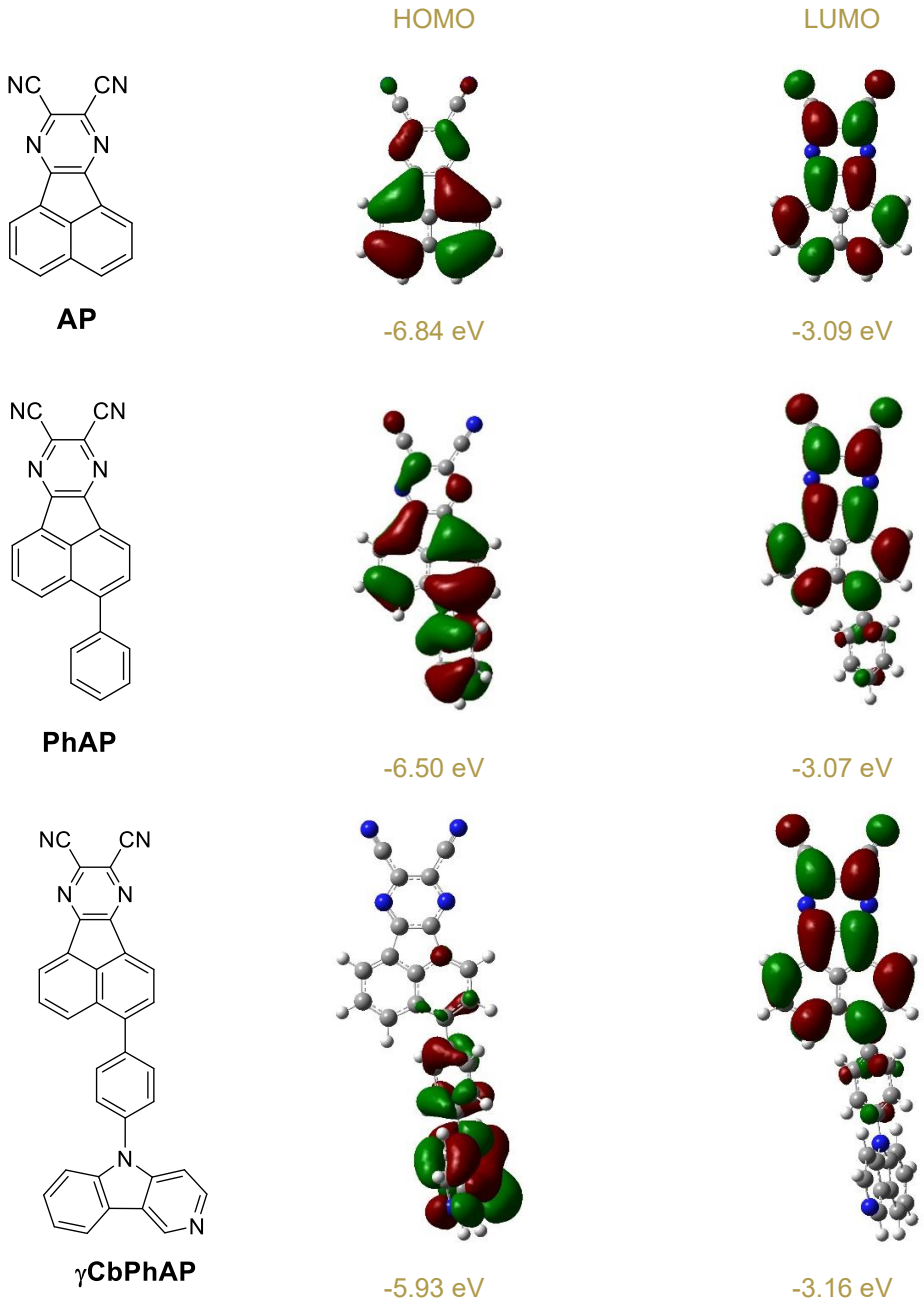

Fig. S15 Calculated energy levels and contour plots of HOMO and LUMO of **AP**, **PhAP** and **γCbPhAP**.

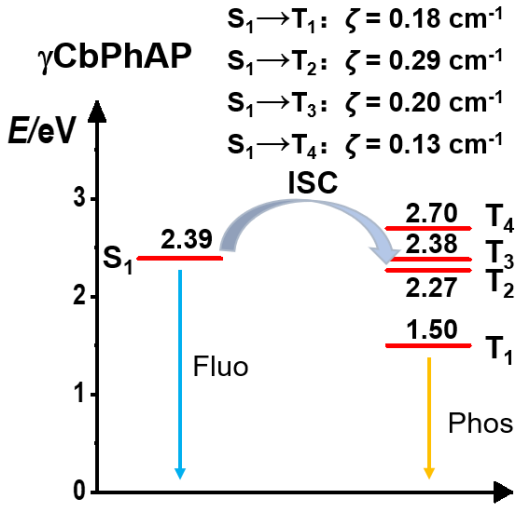

Fig. S16 Calculated S_1 and T_n energy levels and SOC matrix element values between S_1 and T_n states of **γCbPhAP**.

Table S6 Calculated NTO pairs and energy levels of the excited singlet and triplet states of **AP** (PBE0 functional, 6-31g(d) basis set, in Tol).

	Hole	Particle	Transition character	Excitation energy
$S_0 \rightarrow S_1$	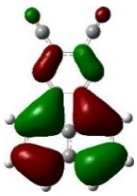	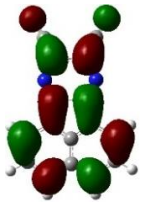	^{1}LE	3.18 eV
$S_0 \rightarrow T_1$	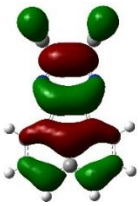	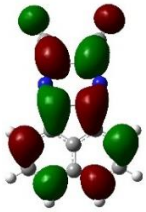	^{3}LE	1.81 eV
$S_0 \rightarrow T_2$	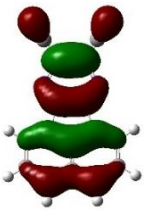	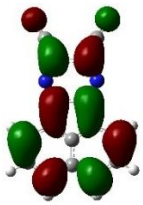	^{3}LE	2.27 eV
$S_0 \rightarrow T_3$	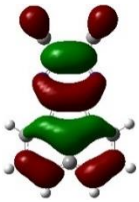	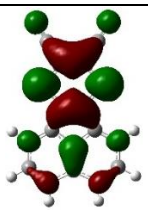	^{3}LE	2.75 eV
$S_0 \rightarrow T_4$	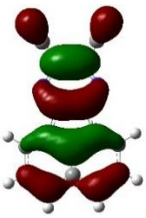	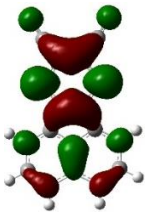	^{3}LE	3.08 eV
$S_0 \rightarrow T_5$	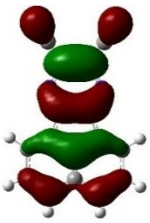	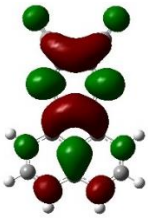	^{3}LE	3.41 eV

Table S7 Calculated NTO pairs and energy levels of the excited singlet and triplet states of **PhAP** (PBE0 functional, 6-31g(d) basis set, in Tol).

	Hole	Particle	Transition character	Excitation energy
$S_0 \rightarrow S_1$	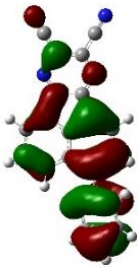	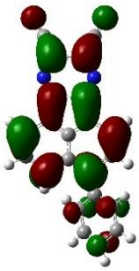	^{1}LE	2.70 eV
$S_0 \rightarrow T_1$	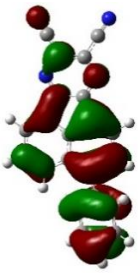	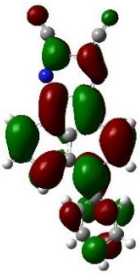	^{3}LE	1.54 eV
$S_0 \rightarrow T_2$	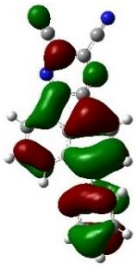	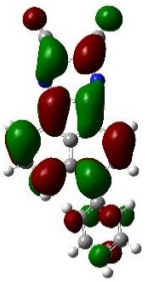	^{3}LE	2.28 eV
$S_0 \rightarrow T_3$	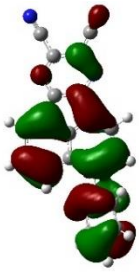	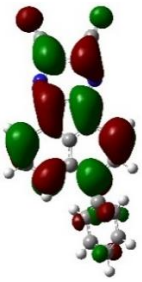	^{3}LE	2.55 eV
$S_0 \rightarrow T_4$	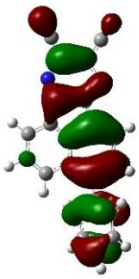	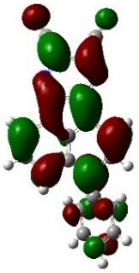	^{3}LE	3.05 eV

Table S8 Calculated NTO pairs and energy levels of the excited singlet and triplet states of **γCbPhAP** (PBE0 functional, 6-31g(d) basis set, in Tol).

	Hole	Particle	Transition character	Excitation energy
$S_0 \rightarrow S_1$	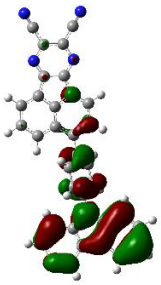	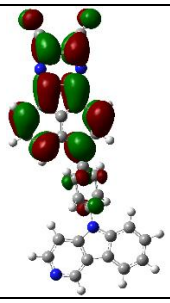	$^1CT_{D\text{-}A}$	2.39 eV
$S_0 \rightarrow T_1$	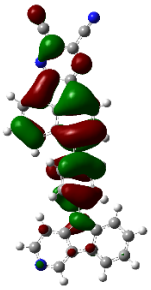	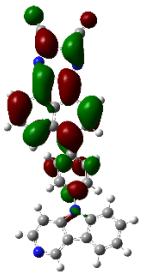	^3LE_A	1.50 eV
$S_0 \rightarrow T_2$	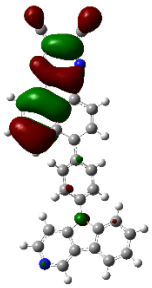	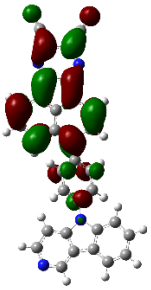	^3LE_A-dominated + ^3CT_A	2.27 eV
$S_0 \rightarrow T_3$	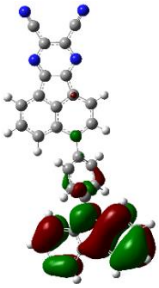	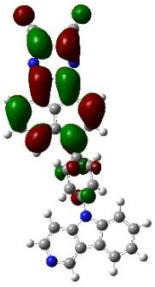	$^3CT_{D\text{-}A}$	2.38 eV
$S_0 \rightarrow T_4$	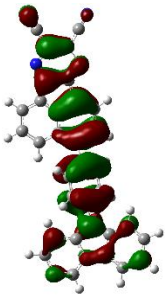	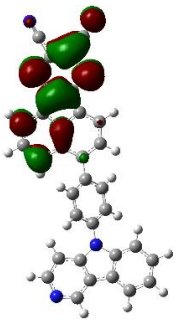	$^3CT_{D\text{-}A}$-dominated + ^3LE_A	2.70 eV

III. ^{1}H NMR, ^{13}C NMR and HRMS spectra

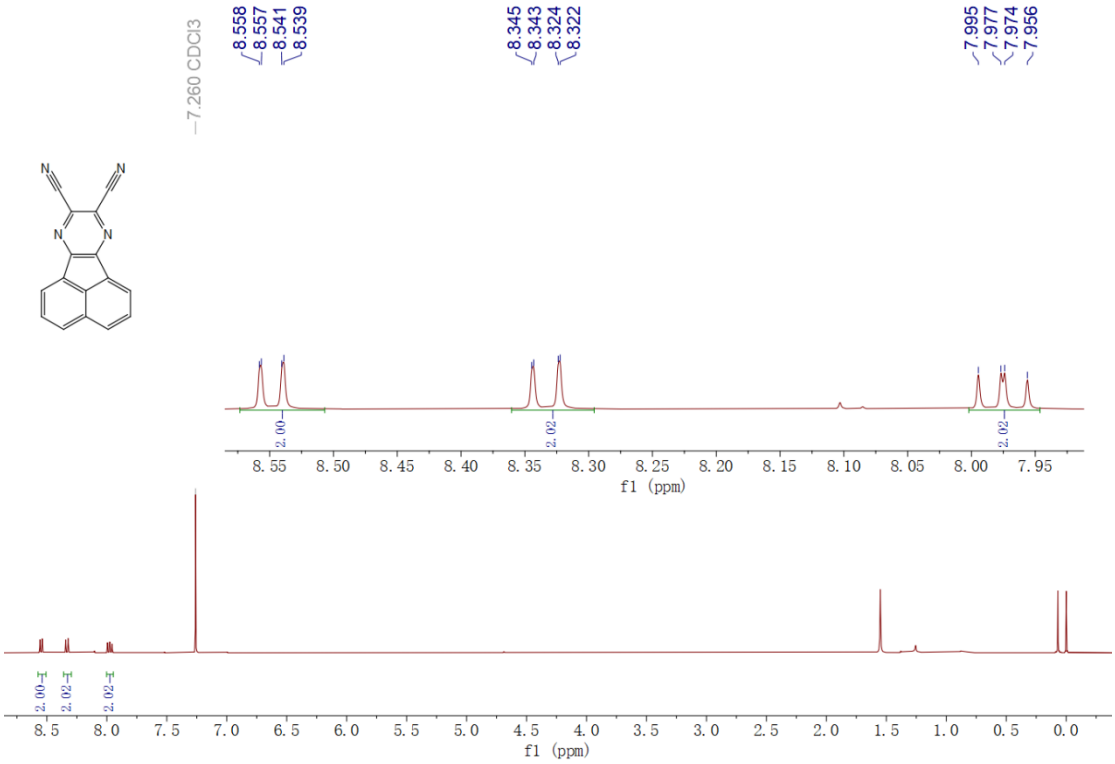

Fig. S17 ^{1}H NMR spectrum of **AP** in $CDCl_3$.

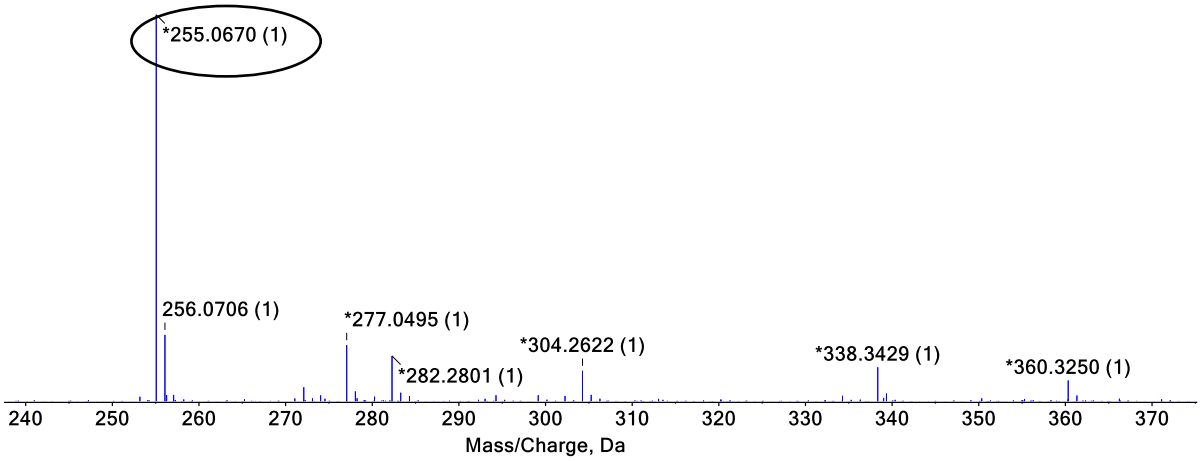

Fig. S18 HRMS spectrum of **AP**.

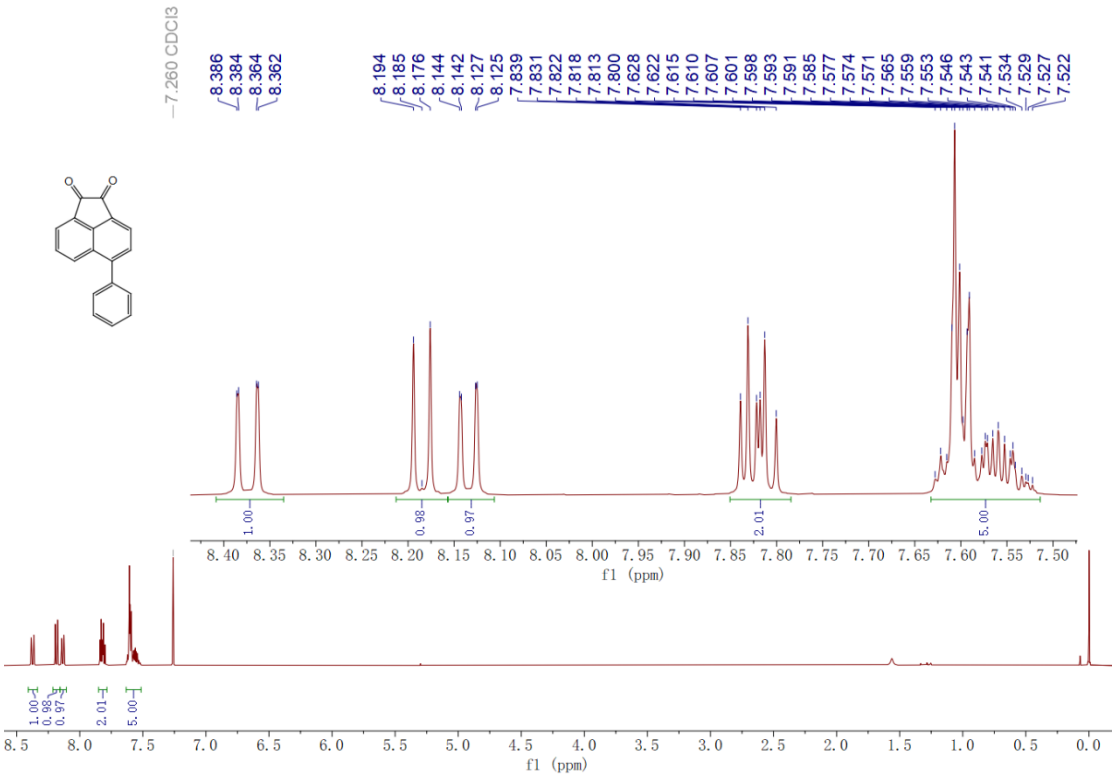

Fig. S19 ^{1}H NMR spectrum of **1** in $CDCl_3$.

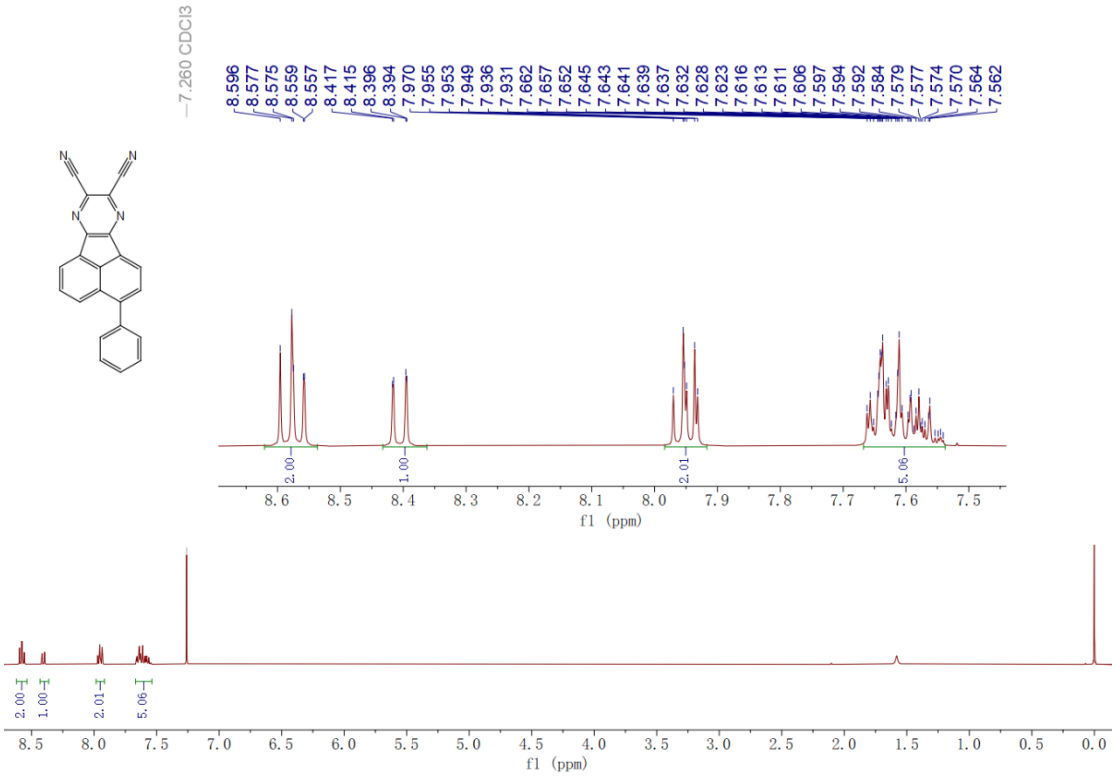

Fig. S20 ^{1}H NMR spectrum of **PhAP** in $CDCl_3$.

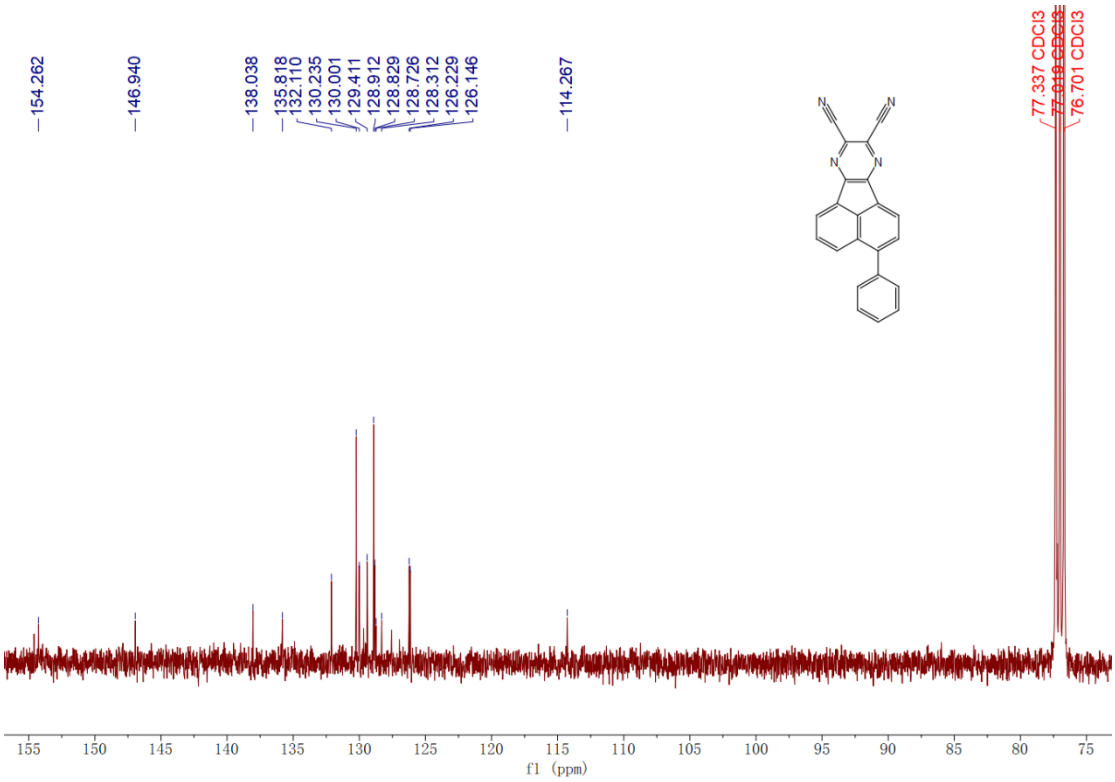

Fig. S21 ^{13}C NMR spectrum of **PhAP** in $CDCl_3$.

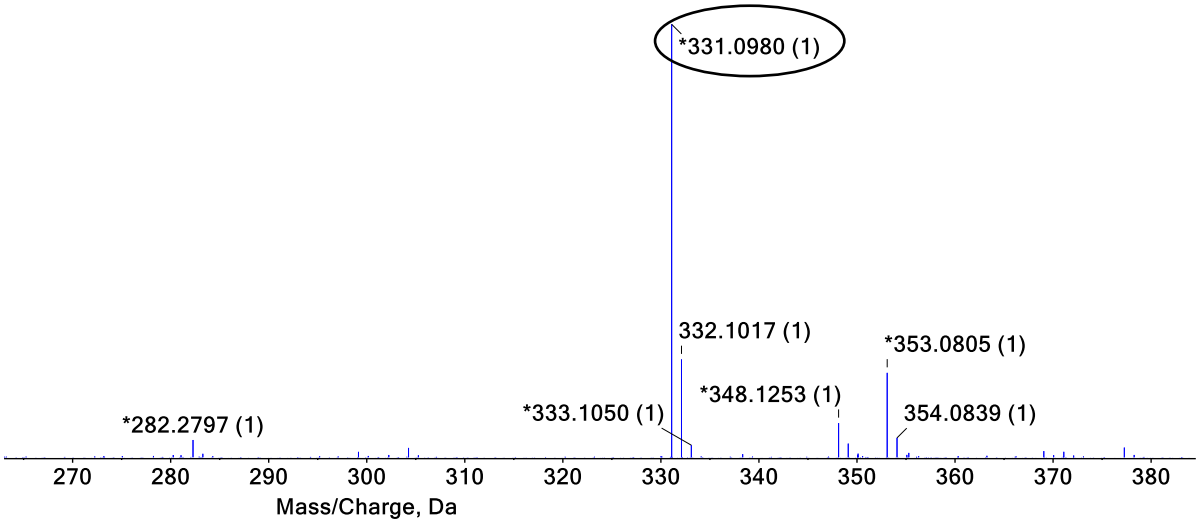

Fig. S22 HRMS spectrum of **PhAP**.

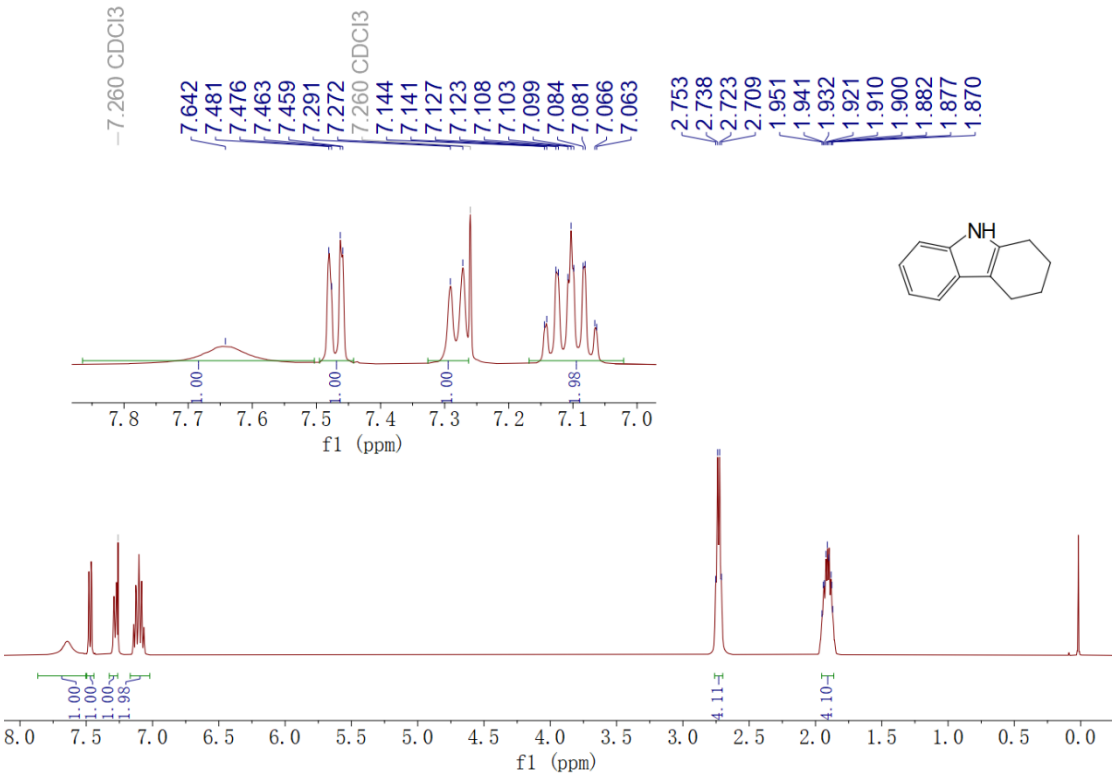

Fig. S23 ^{1}H NMR spectrum of **2** in $CDCl_3$.

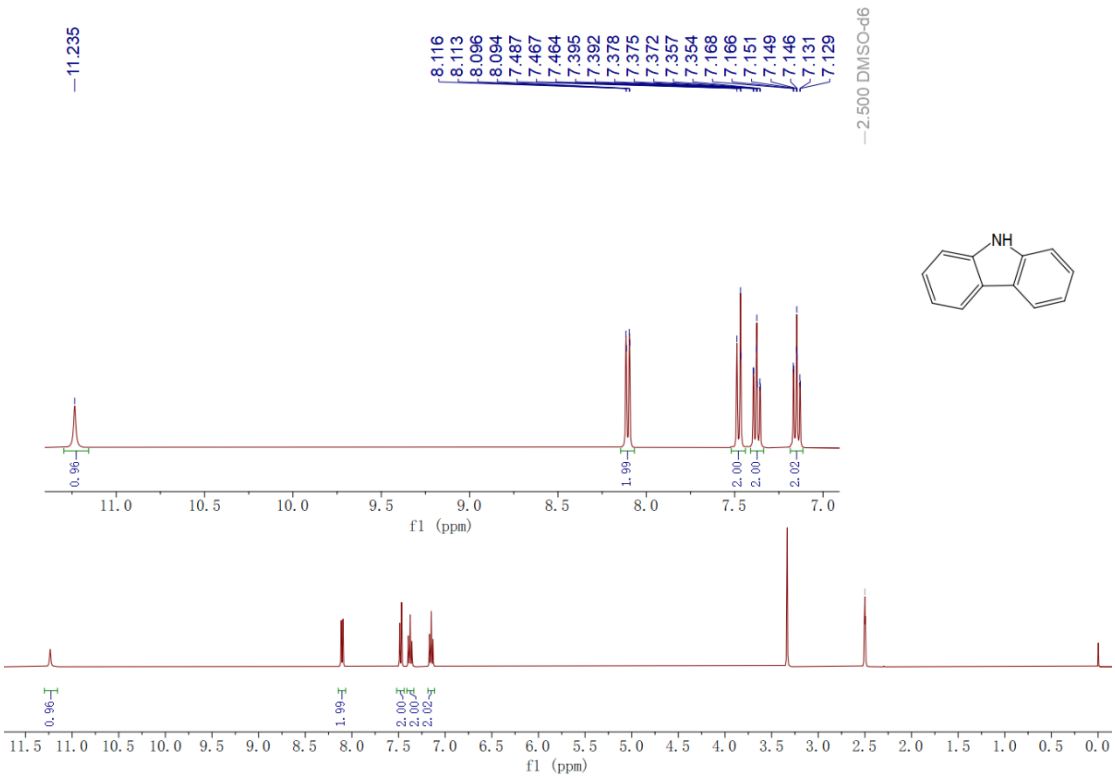

Fig. S24 ^{1}H NMR spectrum of **Cz** in DMSO-d_6.

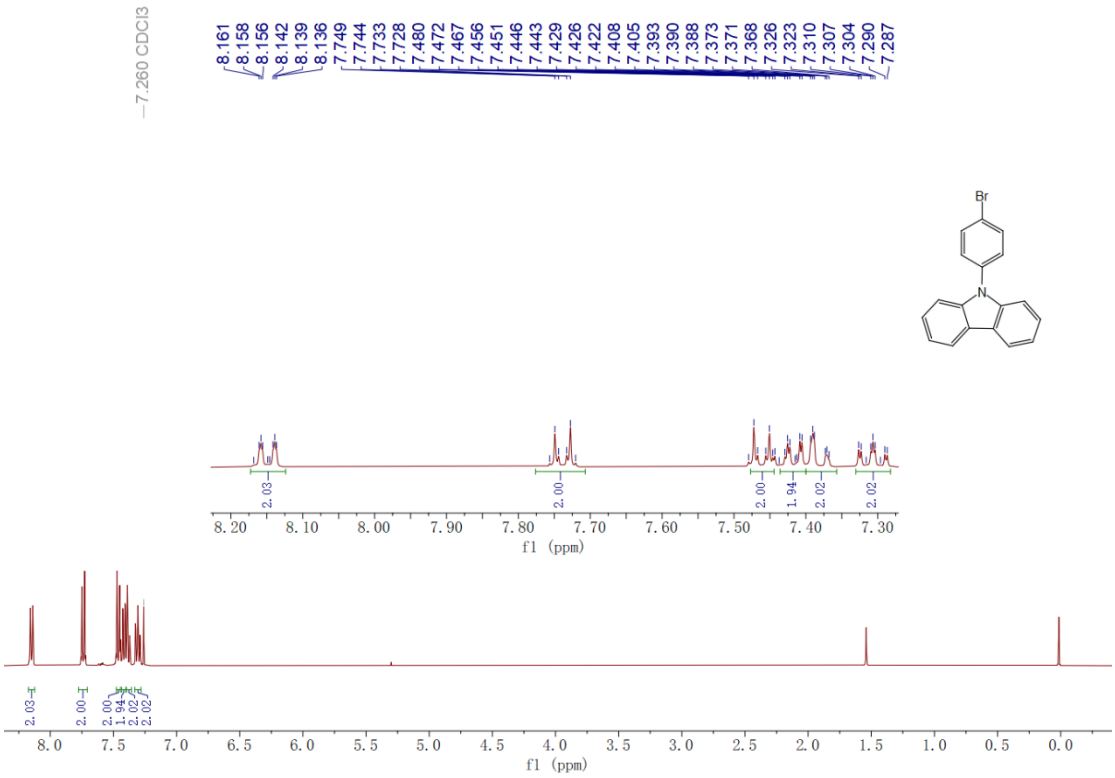

Fig. S25 ^{1}H NMR spectrum of **3** in $CDCl_3$.

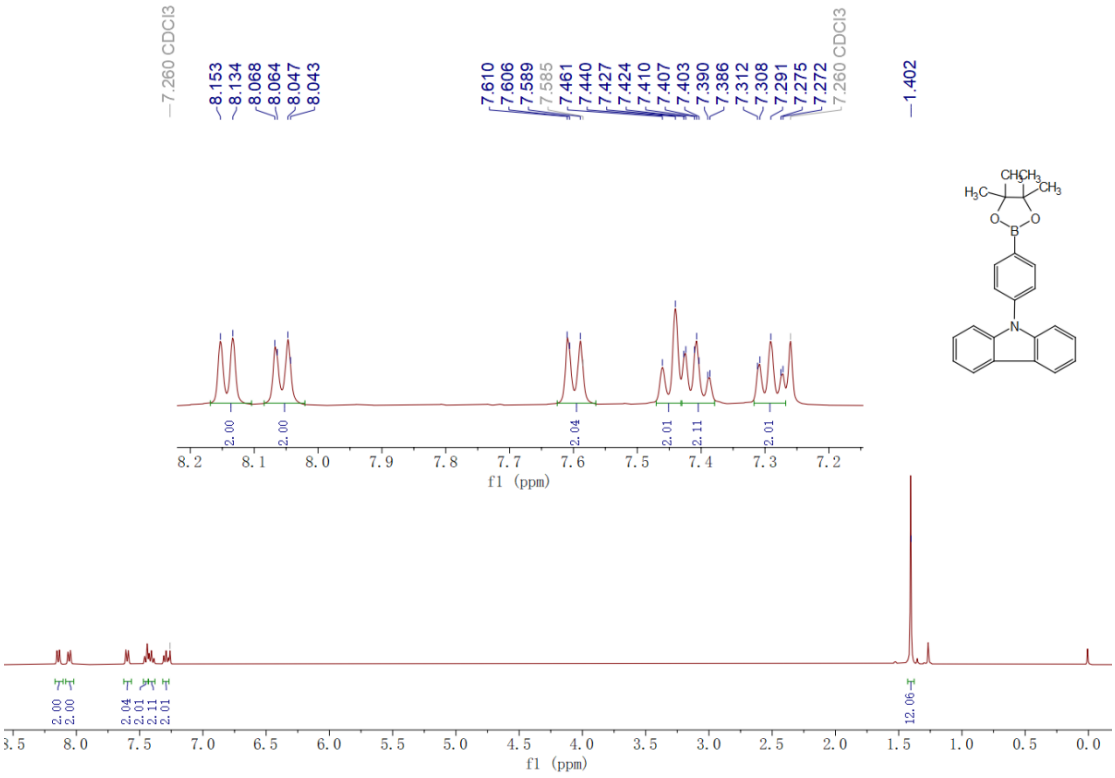

Fig. S26 ^{1}H NMR spectrum of **4** in $CDCl_3$.

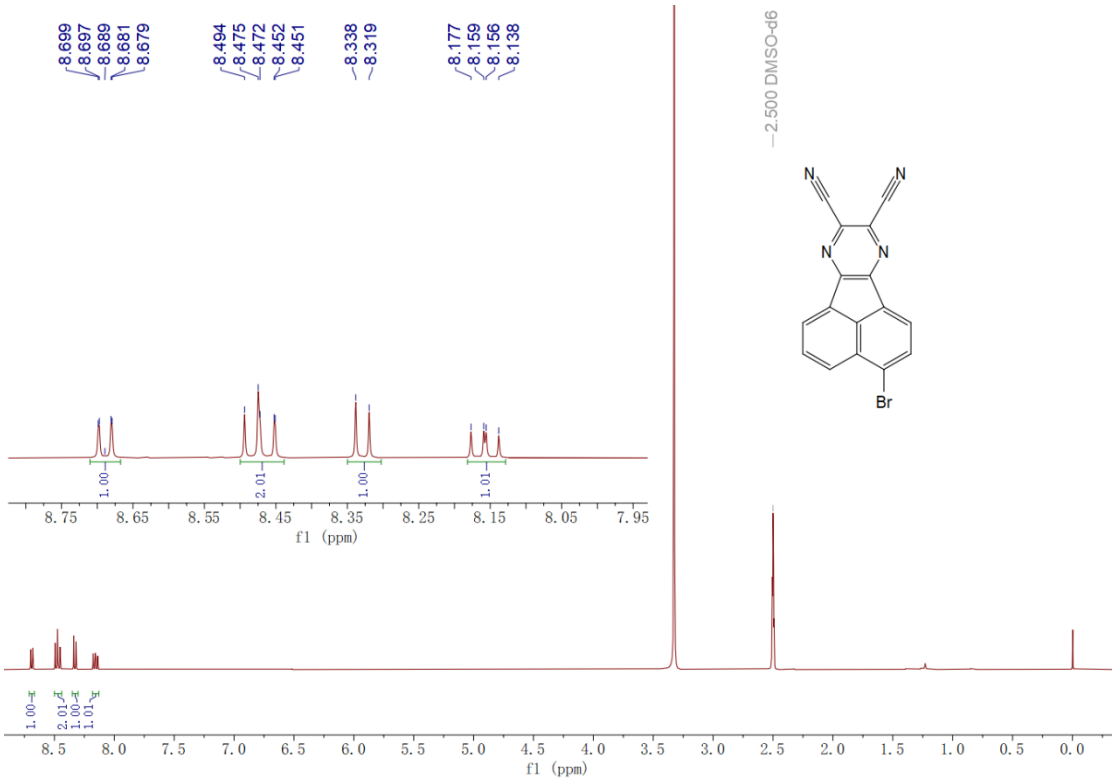

Fig. S27 ^{1}H NMR spectrum of **5** in DMSO-d_6.

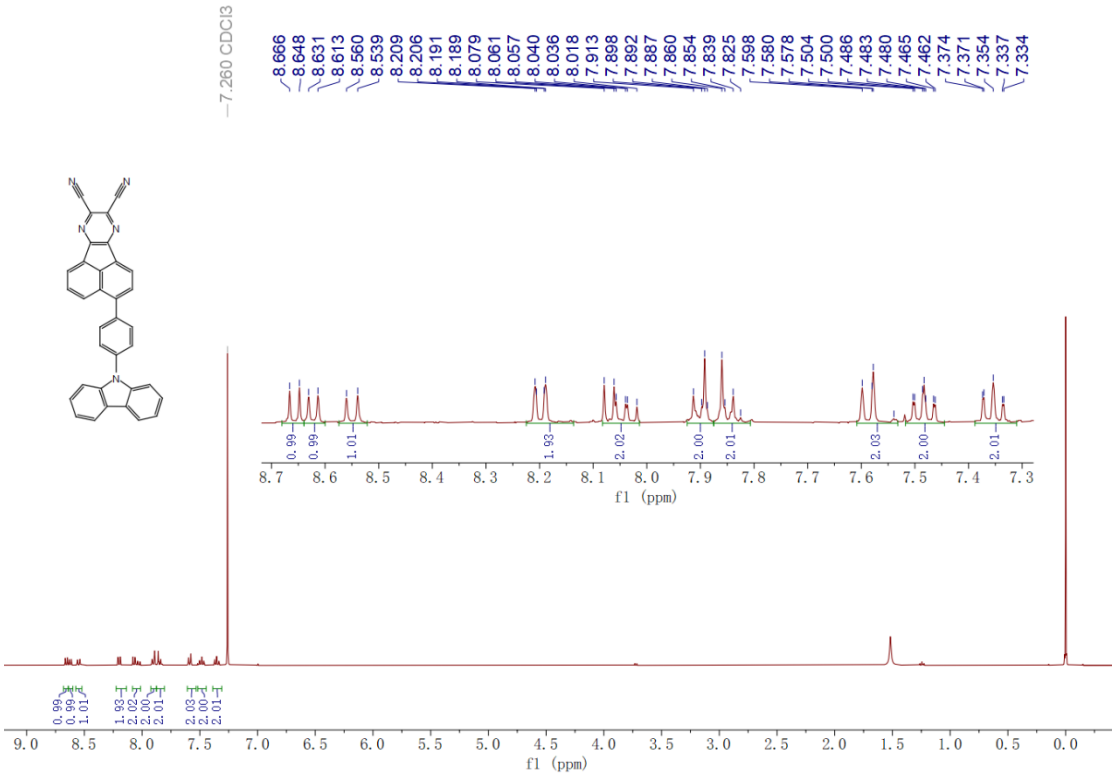

Fig. S28 ^{1}H NMR spectrum of **CzPhAP** in $CDCl_3$.

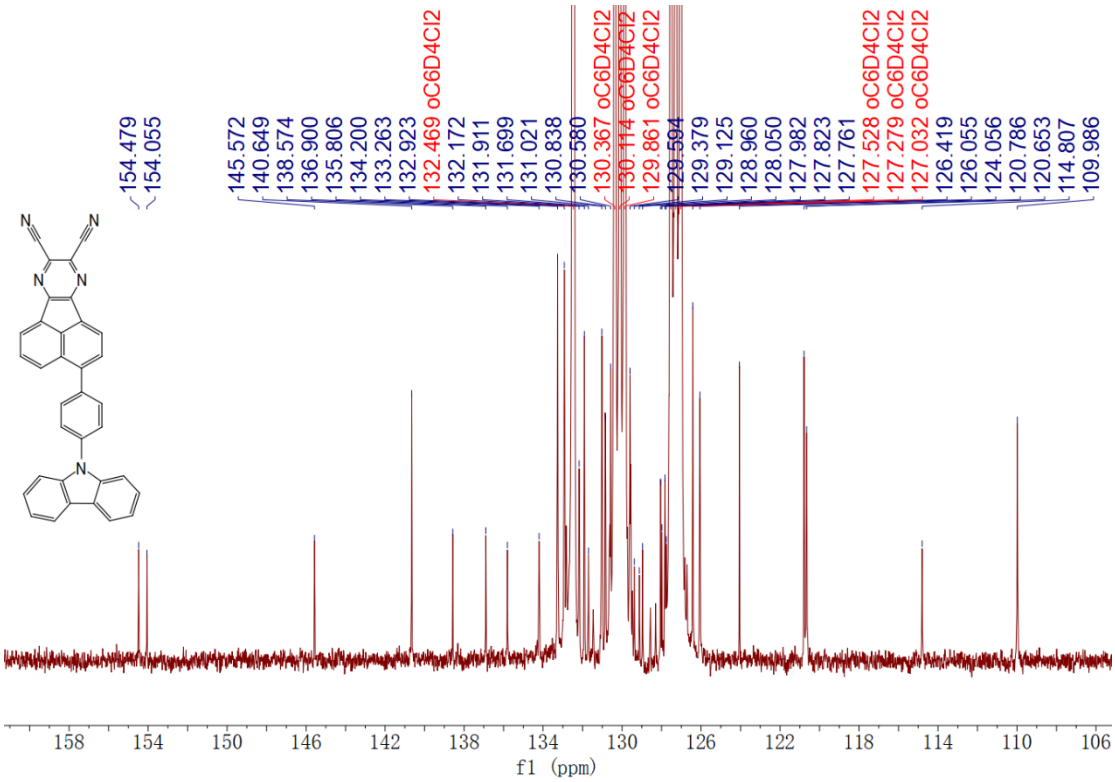

Fig. S29 ^{13}C NMR spectrum of **CzPhAP** in 1,2-dichlorobenzene-d_4.

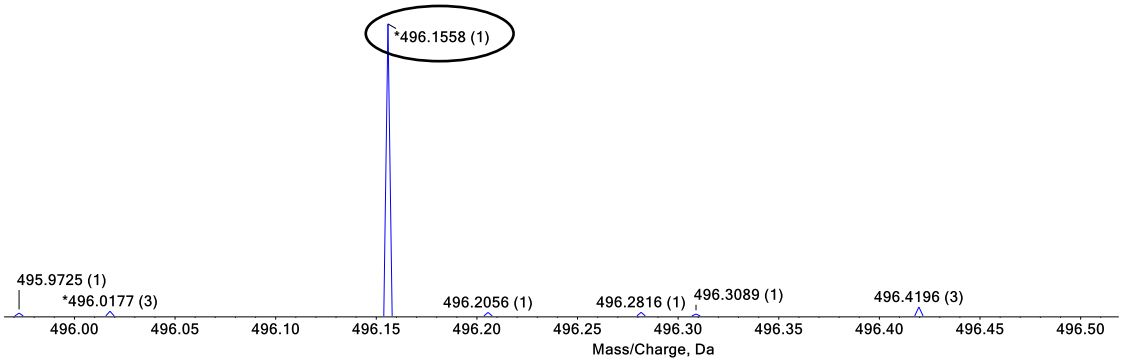

Fig. S30 HRMS spectrum of **CzPhAP**.

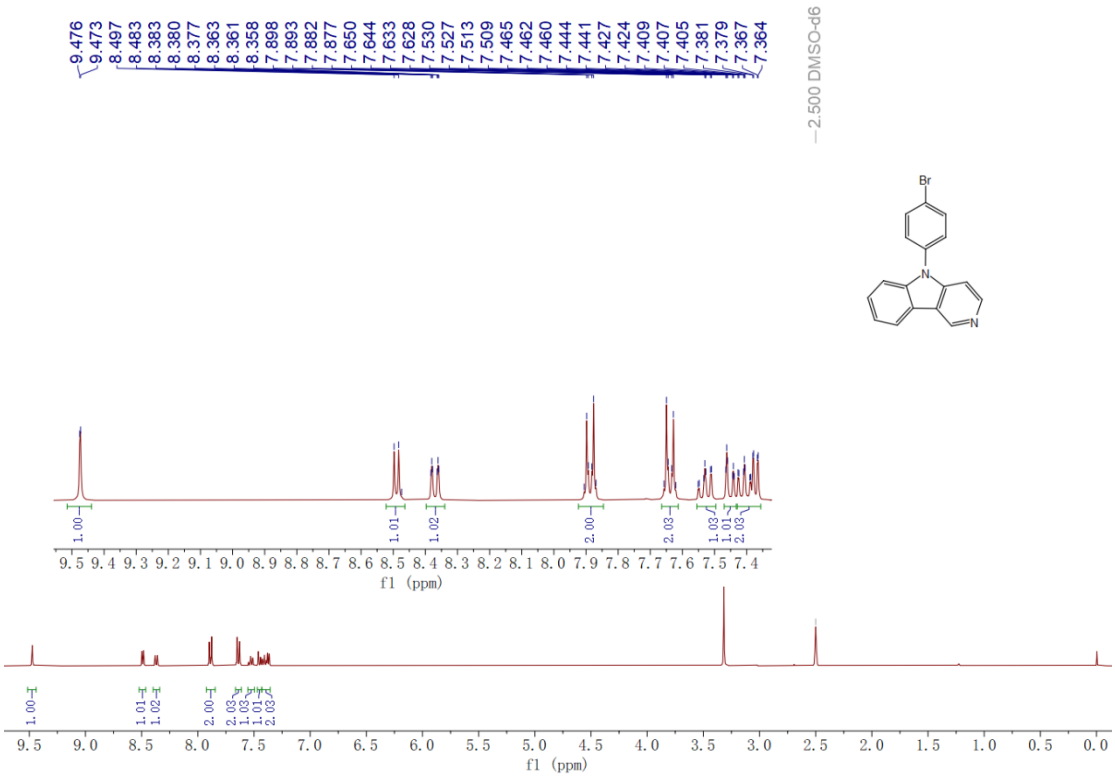

Fig. S31 ^{1}H NMR spectrum of **6** in DMSO-d_6.

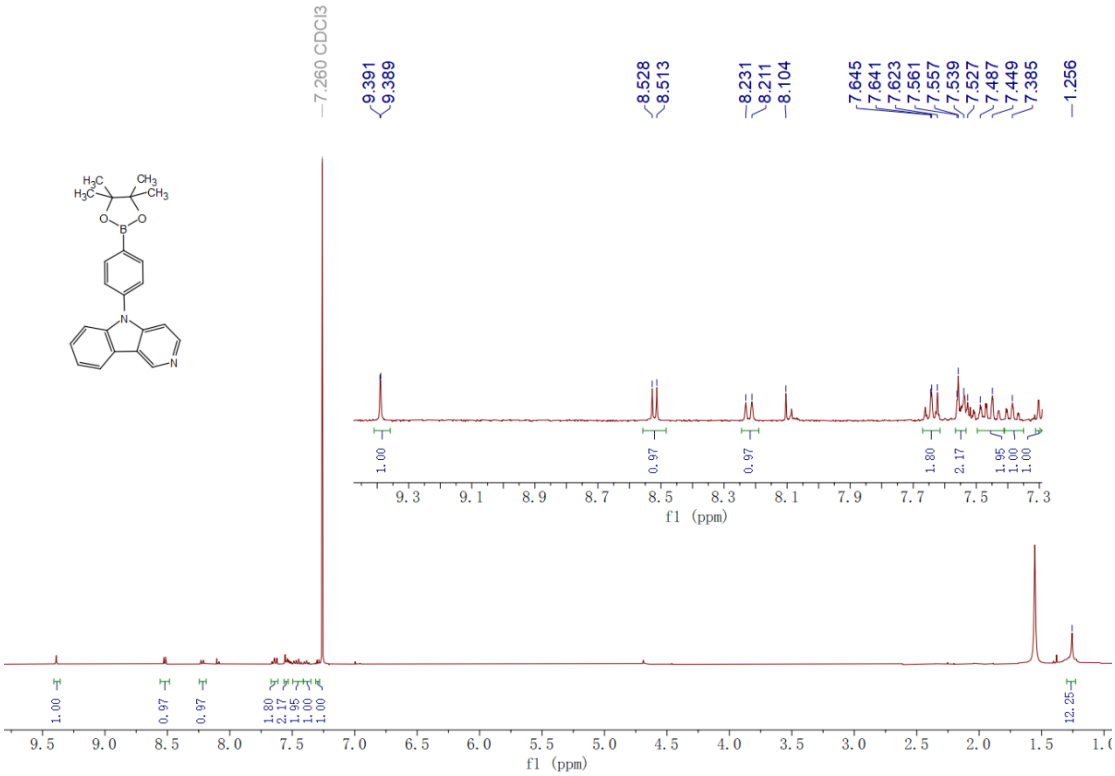

Fig. S32 ^{1}H NMR spectrum of **7** in $CDCl_3$.

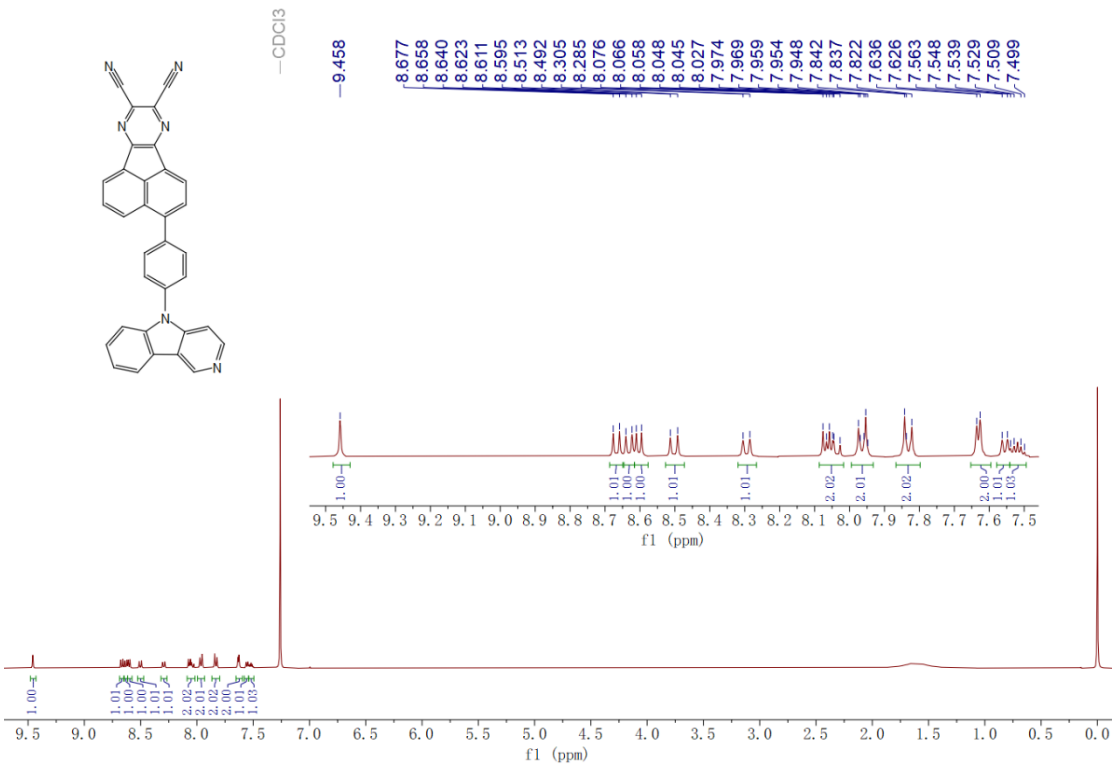

Fig. S33 ^{1}H NMR spectrum of **γCbPhAP** in $CDCl_3$.

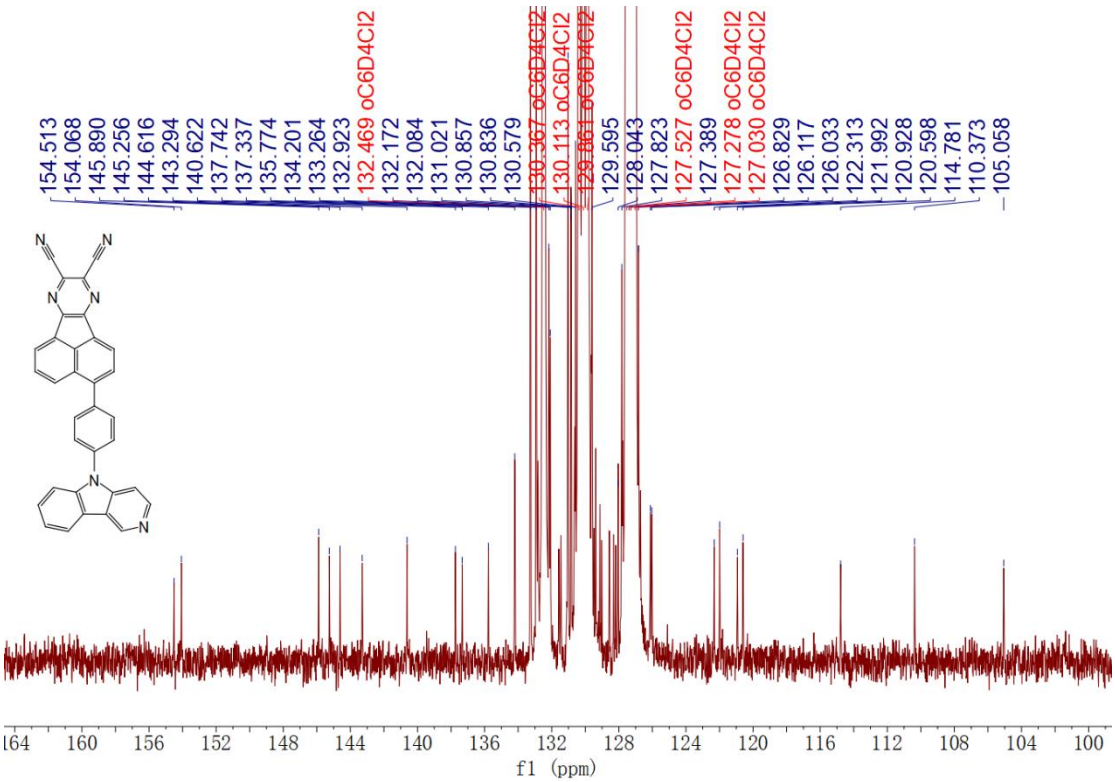

Fig. S34 ^{13}C NMR spectrum of **CzPhAP** in 1,2-dichlorobenzene-d_4.

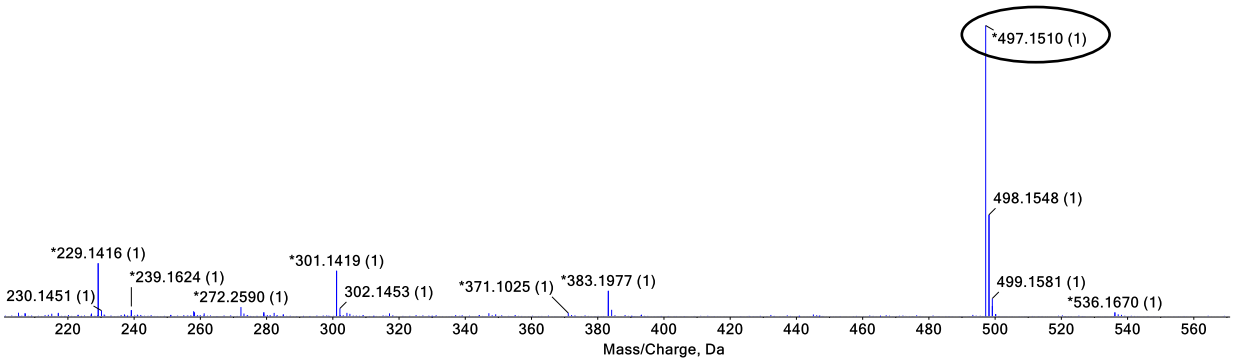

Fig. S35 HRMS spectrum of **γCbPhAP**.

References

1. X. Zheng, Q. Han, Q. Lin, C. Li, J. Jiang, Q. Guo, X. Ye, W. Z. Yuan, Y. Liu and X. Tao, *Mater. Horiz.*, 2023, **10**, 197-208.
2. S. Hirata and M. Vacha, *Adv. Opt. Mater.*, 2017, **5**, 1600996.
3. H. Peng, G. Xie, Y. Cao, L. Zhang, X. Yan, X. Zhang, S. Miao, Y. Tao, H. Li, C. Zheng, W. Huang and R. Chen, *Sci. Adv.*, 2022, **8**, eabk2925.
4. S. Kuila and S. J. George, *Angew. Chem. Int. Ed.*, 2020, **59**, 9393-9397.
5. K. Fukasawa, Y. Sugawara, R. Tsuru, T. Yamashita and S. Hirata, *J. Phys. Chem. Lett.*, 2022, **13**, 7788-7796.
6. Y. Katsurada, S. Hirata, K. Totani, T. Watanabe and M. Vacha, *Adv. Opt. Mater.*, 2015, **3**, 1726-1737.
7. J. Jovaisaite, S. Kirschner, S. Raisys, G. Kreiza, P. Baronas, S. Jursenas and M. Wagner, *Angew. Chem. Int. Ed.*, 2023, **62**, e202215071.
8. J. Zhang, S. Xu, L. Zhang, X. Wang, Y. Bian, S. Tang, R. Zhang, Y. Tao, W. Huang and R. Chen, *Adv. Mater.*, 2022, **34**, 2206712.
9. Y. Lei, W. Dai, J. Guan, S. Guo, F. Ren, Y. Zhou, J. Shi, B. Tong, Z. Cai, J. Zheng and Y. Dong, *Angew. Chem. Int. Ed.*, 2020, **59**, 16054-16060.
10. D. Li, J. Yang, M. Fang, B. Z. Tang and Z. Li, *Sci. Adv.*, 2022, **8**, eabl8392.
11. F. Xiao, H. Gao, Y. Lei, W. Dai, M. Liu, X. Zheng, Z. Cai, X. Huang, H. Wu and D. Ding, *Nat. Commun.*, 2022, **13**, 186.